Changes of neurotransmitter receptor densities in *Crybb2* knock out mouse brains – A model relevant to cataract

Rheinisch-Westfälische Technische Hochschule Aachen
Fakultät für Mathematik, Informatik und Naturwissenschaften

Diese Arbeit wurde im Institut für Neurowissenschaften und Medizin (INM-1) des Forschungszentrums Jülich durchgeführt.

Zur Erlangung des akademischen Grades *Master of Applied Science*

Aachen, den 17.01.2020

Vorgelegt von: Anika Kuckertz
Studiengang: Molekulare und Angewandte Biotechnologie
Matrikelnummer: 381993

Prüfer**:** Univ.- Prof. Dr. Björn Michael Kampa

Rheinisch-Westfälische Technische Hochschule Aachen, Institut der Biologie

Univ.- Prof. Dr. Katrin Amunts

Heinrich-Heine-Universität Düsseldorf, Forschungszentrum Jülich, INM-1

Zentrales Prüfungsamt/Central Examination Office

Eidesstattliche Versicherung
Statutory Declaration in Lieu of an Oath

Kuckertz, Anika 381993
Name, Vorname/Last Name, First Name Matrikelnummer (freiwillige Angabe)
Matriculation No. (optional)

Ich versichere hiermit an Eides Statt, dass ich die vorliegende ~~Arbeit/Bachelorarbeit/~~ Masterarbeit* mit dem Titel
I hereby declare in lieu of an oath that I have completed the present ~~paper/Bachelor thesis/~~ Master thesis* entitled

Changes of neurotransmitter receptor densities in *Crybb2* knock out mouse brains – A model relevant to cataract

selbstständig und ohne unzulässige fremde Hilfe (insbes. akademisches Ghostwriting) erbracht habe. Ich habe keine anderen als die angegebenen Quellen und Hilfsmittel benutzt. Für den Fall, dass die Arbeit zusätzlich auf einem Datenträger eingereicht wird, erkläre ich, dass die schriftliche und die elektronische Form vollständig übereinstimmen. Die Arbeit hat in gleicher oder ähnlicher Form noch keiner Prüfungsbehörde vorgelegen.
independently and without illegitimate assistance from third parties (such as academic ghostwriters). I have used no other than the specified sources and aids. In case that the thesis is additionally submitted in an electronic format, I declare that the written and electronic versions are fully identical. The thesis has not been submitted to any examination body in this, or similar, form.

Jülich, den 16.01.2020 A. Kuckertz
Ort, Datum/City, Date Unterschrift/Signature
*Nichtzutreffendes bitte streichen
*Please delete as appropriate

Belehrung:
Official Notification:
§ 156 StGB: Falsche Versicherung an Eides Statt
Wer vor einer zur Abnahme einer Versicherung an Eides Statt zuständigen Behörde eine solche Versicherung falsch abgibt oder unter Berufung auf eine solche Versicherung falsch aussagt, wird mit Freiheitsstrafe bis zu drei Jahren oder mit Geldstrafe bestraft.
Para. 156 StGB (German Criminal Code): False Statutory Declarations
Whoever before a public authority competent to administer statutory declarations falsely makes such a declaration or falsely testifies while referring to such a declaration shall be liable to imprisonment not exceeding three years or a fine.
§ 161 StGB: Fahrlässiger Falscheid; fahrlässige falsche Versicherung an Eides Statt
(1) Wenn eine der in den §§ 154 bis 156 bezeichneten Handlungen aus Fahrlässigkeit begangen worden ist, so tritt Freiheitsstrafe bis zu einem Jahr oder Geldstrafe ein.
(2) Straflosigkeit tritt ein, wenn der Täter die falsche Angabe rechtzeitig berichtigt. Die Vorschriften des § 158 Abs. 2 und 3 gelten entsprechend.
Para. 161 StGB (German Criminal Code): False Statutory Declarations Due to Negligence
(1) If a person commits one of the offences listed in sections 154 through 156 negligently the penalty shall be imprisonment not exceeding one year or a fine.
(2) The offender shall be exempt from liability if he or she corrects their false testimony in time. The provisions of section 158 (2) and (3) shall apply accordingly.
Die vorstehende Belehrung habe ich zur Kenntnis genommen:
I have read and understood the above official notification:

Jülich, den 16.01.2020 A. Kuckertz
Ort, Datum/City, Date Unterschrift/Signature

Table of contents

Abbreviations

[^{3}H]	tritium
AMPA	α-amino-3-hydroxy-5-methyl-4-isoxazol-propionic acid
BZ	benzodiazepine
CA1; CA2/3	cornu ammonis 1 and 2/3, hippocampus
cAMP	cyclic adenosine monophosphate
Cb	cerebellum
CO_2	carbon dioxide
CPu	caudate putamen, striatum
Crybb2	βB2-crystallin gene
Crybb2^{O377}	the study relevant cataract mouse model
$D_{2/3}$	dopamine receptor subtype 2/3
DG	dentate gyrus, hippocampus
DPX	dibutylphthalate polystyrene xylene
GABA	γ-aminobutyric acid
G-protein	guanine nucleotide-binding protein
INM-1	Institute of Neuroscience and Medicine
M1	primary motor cortex
$mGlu_{2/3}$	metabotropic glutamate receptor subtype 2/3
NMDA	N-methyl-D-aspartate
OB	olfactory bulb
p_{uc}	p-value$_{uncorrected}$
S1	somatosensory cortex
SD	standard deviation
V1	primary visual cortex

Abstract

Age-related cataract is one of the most common cause of vision decline and could be associated to structural and functional impairments of the brain. The causal link between the disease and mutations of crystalline genes as well as the resulting protein structure changes is well known.

The aim of the present study was to investigate mean densities and distribution patterns of eight neurotransmitter receptors (AMPA, kainate, NMDA, $mGlu_{2/3}$, $GABA_A$, BZ, $GABA_B$ and $D_{2/3}$) in the brains of *Crybb2*^{O377} compared to control mice, by means of quantitative *in vitro* receptor autoradiography.

Receptor distribution patterns were similar between cataract and wild type animals for all receptor types and brain regions investigated. No significant changes between receptor densities of both groups could be found based on statistics including correction for multiple comparisons. However, differential nominally significant results of changed densities for kainate, $GABA_A$ and $GABA_B$ receptors could be determined.

A tended increase of kainate as well as $GABA_B$ receptor densities were shown for the visual cortex of cataract mice. This could indicate possible compensatory processes for the maintenance of neuronal function and the synaptic plasticity in the potentially affected visual cortex of *Crybb2*^{O377} mice. Additionally, $GABA_A$ receptors exhibited tendencies of decreased densities in the olfactory bulb, the somatosensory cortex and the hippocampal CA1 region of *Crybb2*^{O377} mice. These receptor downregulations could also represent compensatory mechanisms with respect to inhibitory chloride currents in order to maintain excitability in cataract-affected neurons.

In sum, the results of the present study indicate differential trends of altered neurotransmitter receptor densities in the brains of *Crybb2*^{O377} mice compared to corresponding controls. These provided novel data for possible neurological compensations due to cataract in early development. Thus, kainate, $GABA_A$ and $GABA_B$ receptors as well as the respective neurotransmitter systems in general, have been identified as interesting targets for future studies.

1 Introduction

1.1. Age-related cataract

Age-related cataract is a vision-impairing disease that is characterized by progressive clouding of the eye lens. According to an extrapolation of the `International Centre for Eye Health´, age-related cataract will affect around 800 million people aged over 60 years in 2020 (Allen Foster, 2000). The rising tendency of cataract patients points out the importance for a comprehensive understanding of the disease, ideally enabling improved possibilities for diagnosis and therapy.

Age-related cataract occurs between an age of 45 and 60 years and the prevalence of cataract appearance rises with age (Ueda et al., 2002). Major pathogenic factors for the development of cataract are age-related changes and aggregation of lens proteins (Lampi et al., 1998). The most abundant eye lens proteins are crystallins (Bateman et al., 2003; Chen et al., 2013), which represent about 90 % of the vertebrate eye lens content (Wistow and Piatigorsky, 1988; Chen et al., 2013). Crystallins can be subdivided into three main classes, α- ,β- and γ-crystallins, based on their characteristic amino acid compositions and polypeptide chains (Brady et al., 1997). The present study focused on the most prominent βB2-crystallins (Bax et al., 1990).

The most important feature of crystallins is the water-solubility, which is required for permanent lens clarity and the high refraction index of the eye lens (Bateman et al., 2003; Zhang et al., 2008). βB2-crystallins play an essential role in maintaining the water-solubility because of extensive intramolecular protein interactions (Trinkl et al., 1994). During aging as well as in the development of cataract, protein structures of crystallins are altered by additional posttranslational protein modifications i.e. phosphorylation and deamination (Lampi et al., 1998; Zhang et al., 2008). Consequently, the interactions of the resulting modified protein structures are affected, leading to the formation of insoluble crystallin aggregates (Chambers and Russell, 1991; Lampi et al., 2014). In particular, the aggregation and accumulation of disrupted βB2-crystallins was described as one critical reason for the development of lens opacity in age-related cataract (Ueda et al., 2002; Zhang et al., 2008).

Formation of insoluble crystallin aggregates results in the cataract phenotypic opacity, mostly spreading from the center of the lens to the periphery (Ueda et al., 2002). Lens

opacity reduces the refraction of incident light and affects light focusing onto the retina (Lampi et al., 1998), which is a reason for light scattering and thus the visual impairment of cataract patients (Brady et al., 1997).

Age-related cataract was described as major reason for visual impairment that could be associated to cognitive decline and abnormal changes in the brain structure, especially in the older population (Lin et al., 2018; Maharani et al., 2018). Neurotransmitters as well as their respective receptors play a decisive role for the function and thus also the structure of the brain. In the present study, three classical neurotransmitter systems were investigated, regarding their regional localization as well as quantitative presence in brains of cataract-affected and healthy mice.

1.2. *Crybb2*^{O377} – A mouse model of cataract

βB2-crystallins are the most abundant as well as least modified crystallins and exhibit extensive protein interactions (Trinkl et al., 1994). These two facts lead to the assumption, that βB2-crystallins play a major role in maintaining the water-solubility necessary for lens clarity (Zhang et al., 2008; Chen et al., 2013). The O377 mouse model (*Crybb2*^{O377}) of age-related cataract is characterized by a point mutation in the βB2-crystallin gene (*Crybb2*), which leads to the formation of insoluble βB2-crystallin aggregates (Graw, 2009). Mutational-dependent, as well as cataract-associated affected βB2-crystallin folding was described as a critical reason for the development of lens opacity and cataract (Ueda et al., 2002).

The homozygous *Crybb2*^{O377} mice analyzed in the present study were established and described by Graw et al., 2009 (Graw, 2009). In detail, the O377 cataract mutation is based on a transversion from adenine to thymidine in a specific position of *Crybb2*, which leads to the insertion of a 57 bp mRNA sequence. This sequence forms an additional peptide loop result in affected protein folding and the formation of insoluble βB2-crystallin lens aggregates, which cause the cataract-phenotypic lens opacity (Ganguly et al., 2008; Graw, 2009; Sun et al., 2013).

In *Crybb2* knock out mice lens opacity starts after 6 to 8 weeks of age, continues progressively with age, and is completely developed after 18 months (Zhang et al., 2008). Additional to an assumed lens opacity, *Crybb2*^{O377} mice seemed to exhibit

behavioral alterations i.e., spending more time in social investigations. Furthermore, no olfactory deficits could be observed in *Crybb2*^{O377} mice (Sun et al., 2013).

1.3. Receptor autoradiography & neurotransmitter systems

Neurotransmitters and their receptors are decisive elements of neuronal signal transduction and thus play an important role for cognitive function. Previous studies showed differential alterations of neurotransmitter systems in neurological and psychiatric disorders of humans, as well as in corresponding animal models (Zilles et al., 1999; Cremer et al., 2015a; Cremer et al., 2015b). Additionally, neurotransmitters are clinically relevant, since their specific binding sites are frequently used as pharmacological targets for the treatment of neurological and psychiatric disorders (Sakurai et al., 1991; Corti et al., 2007).

The method of choice of the present study is the quantitative *in vitro* receptor autoradiography that is based on a specific receptor binding procedure, using tritium-labeled ligands to visualize and quantify neurotransmitter binding sites (Zilles et al., 2002b; Zilles et al., 2002a). Differential alterations of neurotransmitter receptor densities could be observed in ocular diseases (Boroojerdi et al., 2001; Moreno et al., 2008) In the present study, glutamatergic (AMPA, kainate, NMDA, $mGlu_{2/3}$), GABAergic ($GABA_A$, BZ, $GABA_B$) and dopaminergic ($D_{2/3}$) receptors were investigated regarding possible alterations of receptor densities as well as distribution patterns in *Crybb2*^{O377} mice compared to corresponding wild types.

Glutamate is the major excitatory neurotransmitter in the mammalian brain (Nusser et al., 1994; Plested and Mayer, 2007). In the present study, we investigated ionotropic AMPA (α-amino-3-hydroxy-5-methyl-4-isoxazol-propionic acid), kainate and NMDA (N-methyl-D-aspartate) receptors as well as the metabotropic glutamate receptor subtype 2/3 ($mGlu_{2/3}$) (Scheefhals and MacGillavry, 2018).

Activation of ionotropic glutamate receptors results in the opening of glutamate-gated cation (i.e. sodium, calcium) channels (Plested and Mayer, 2007). The resulting depolarization of the neurons initiates different excitatory pathways, e.g. in the context of synaptic plasticity mechanisms (Traynelis et al., 2010), including the formation of neuronal connections i.e., in the visual system (Hollmann and Heinemann, 1994;

Kumar et al., 1994) or learning and memory processes (Kato et al., 2010). On the other hand, metabotropic glutamate receptors are coupled to G-proteins and activation of respective receptors results in different inhibitory effects, e.g. on adenylyl cyclase and calcium channel activity (Chavis et al., 1994; Niswender and Conn, 2010). Inhibitory effects are also involved in mechanisms of synaptic plasticity, amongst others in the context of eye-specific neuronal connections (Reid et al., 1996; Cartmell and Schoepp, 2000).
In a pathologic condition, glutamate receptor overstimulation could lead to excitotoxic calcium levels, which were mentioned in the context of neurological and psychiatric disorders (Choi, 1988; Cartmell and Schoepp, 2000). Furthermore, glutamate receptors are used as targets for pharmaceutical intervention in the treatment of neurological and psychiatric disorders (Corti et al., 2007; De Filippis et al., 2015).

γ-Aminobutyric acid (GABA) is considered as the major inhibitory neurotransmitter in the mammalian brain (Hand et al., 1997; Cancedda et al., 2007). In general, GABA receptors include subgroups of ionotropic $GABA_A$ receptors and $GABA_A$ associated benzodiazepine binding sites, as well as metabotropic $GABA_B$ receptors.

Binding of GABA to its ionotropic receptors triggers depolarization of the neurons and mediates inhibitory signal transmission (Chen, 2014). The GABAergic system affects cognitive processes which including e.g. visual perception (Iversen et al., 1971; Cherubini and Conti, 2001). Ionotropic $GABA_A$ receptors exhibit different subunit compositions for the assembly of chloride permeable channels (Müller Herde et al., 2017). Channel opening and the respective increase of chloride currents can inhibit the firing of neuronal synapses (Cherubini et al., 1991). Under pathological conditions, disrupted chloride channels seem to be involved in the development of opaque lenses (i.e., in cataract) (Zhang et al., 1994). Benzodiazepine (BZ) binding to $GABA_A$ receptors results in an allosteric modulation of GABA-mediated chloride currents and therefore changes in respective signal transmission (Sigel and Buhr, 1997).
$GABA_B$ coupled G-protein receptors modulate several neuronal processes mainly through different inhibitory actions, e.g. on adenylyl cyclase activity and calcium channels (Guyon and Leresche, 1995; Nishikawa et al., 1997). These effects of metabotropic $GABA_B$ receptors regulate, amongst others, mechanisms of synaptic plasticity, which is required for individual modulation of neuronal connections in several

cognitive processes, including learning and memory as well as visual perception (Boroojerdi et al., 2001; Chalifoux and Carter, 2010; Benke et al., 2012).

Dopamine receptors are G-protein coupled and predominantly located on striatal neurons (Stoof, 1988; Boschen et al., 2011). Inhibitory effects, e.g. on adenylyl cyclase and calcium channel activity and resulting neuronal responses, e.g. changed synaptic plasticity of the dopamine receptor subtype 2/3 ($D_{2/3}$) (Onali et al., 1985). To date, little is known about the involvement of dopamine receptors in visual perception

2 Aim of the study

The aim of the present study was to investigate alterations of neurotransmitter receptor densities and distribution patterns in cataract-affected *Crybb2*^{O377} and corresponding wild type mice, by means of quantitative *in vitro* receptor autoradiography. In detail, densities and distribution patterns of eight receptor types of three neurotransmitter systems (Glutamatergic: AMPA, kainate, NMDA, $mGlu_{2/3}$; GABAergic: $GABA_A$, BZ, $GABA_B$ and Dopaminergic: $D_{2/3}$) were investigated in nine brain regions (olfactory bulb, motor and somatosensory cortex, striatum, visual cortex, hippocampal CA1, CA2/3, DG and cerebellum) in order to obtain a comprehensive overview of neurotransmitter receptor expression in this mouse model of cataract

Ocular diseases have been shown to contribute to cognitive decline and abnormal changes in brain structure (Lin et al., 2018). The increasing prevalence of age-related cataract (Allen Foster, 2000) along with the causal link to changes in βB2-crystallins emphasizes the importance of a comprehensive understanding of the pathological changes associated with the disease as well as the underlying mechanisms. This knowledge could provide the foundation required for the improvement of both, possibilities for diagnosis and therapy. The present study was focused on the analysis of neurotransmitter receptors, thereby enabling a comprehensive overview of one crucial aspect of neuronal signal transduction in an animal model of cataract.

3 Materials and Methods

3.1. Animals

All experiments were performed in accordance to the German animal welfare act and approved by the responsible governmental agency, LANUV NRW (Landesamt für Natur, Umwelt und Verbraucherschutz NRW).
Brains of 4-5 months old mice were generously provided by Prof. Dr. med. Jochen Graw (Institute of Developmental Genetics, Helmholtz Center Munich, Germany). For the autoradiographic investigations we used homozygous male *Crybb2*^{O377} mice (n=10) and corresponding male control mice (n=9). Brain sectioning and the autoradiographic analysis of all 19 mice brains, were performed in the Institute of Neuroscience and Medicine 1 (Forschungszentrum Jülich, Germany).

3.2. Preparation of tissue and slices

The mice were anesthetized using carbon dioxide (CO_2) and subsequently decapitated. After immediate dissection, the brains were frozen in isopentane at -70 °C, stored on dry ice and delivered to Forschungszentrum Jülich. Subsequently, the brains were stored at -80 °C.

The frozen and unfixed brains were embedded in Tissue Tec (Sakura, Finetek Germany GmbH), and blocked on a specimen holder. Coronal serial slices (thickness 10 µm) were prepared with a cryostat microtome (Leica Biosystems Vertrieb GmbH, Mikroskopie und Histologie, Wetzlar, Germany) at -15 °C. The brain tissue slices were thaw-mounted on silanized microscope glass slides (Starfrost, 76x26 mm, Germany), dried on a heating plate, and stored in vacuum-sealed plastic boxes at -80 °C. Alternating slices were used for histological staining (cresyl violet) or receptor autoradiography, respectively.

3.3. Receptor autoradiography

In the present study, receptor densities of three different neurotransmitter systems were examined using quantitative *in vitro* receptor autoradiography (glutamatergic receptors: AMPA, kainate, NMDA and $mGlu_{2/3}$; GABAergic receptors: $GABA_A$, $GABA_A$ associated benzodiazepine binding sites and $GABA_B$; dopaminergic receptor: $D_{2/3}$) (Zilles et al., 2002b; Zilles et al., 2002a).

In general, the autoradiographic labeling method consists of three steps. The pre-incubation step, the main incubation with [^{3}H]-labeled ligands and the washing step. The receptor-specific autoradiography protocols are summarized in table 1, including the [^{3}H]ligand work concentrations, the composition of the buffer solutions and the duration of pre-/ main incubation as well as washing steps. The day before a respective binding experiment, the frozen and unfixed tissue slices were pre- warmed at room temperature and the buffers were prepared and stored at 4 °C.

The binding procedure started with the **pre-incubation** in buffer solution, which took 15 to 30 min. After this rehydrating step, endogenous receptor binding substances were washed out. Thus, the binding sites were available for the receptor specific [^{3}H]-labeled ligands(Zilles et al., 2002a).

In the **main incubation** the sections were incubated in buffer solution containing specific working concentrations of a respective [^{3}H]ligand. The actual ligand working concentration was controlled in the Liquid Scintillation Counter 300 SL (Hidex, Finland). In a parallel approach of the main incubation a non-radioactive competitor (about a thousand times higher concentrated) was added to some of the tissue slices to measure unspecific receptor binding (Scheperjans et al., 2005). After a competition for the receptor binding site, the highly affine competitor displaces the [^{3}H]ligand (Zilles et al., 1986). Thus, the nonspecific, and therefore non-displaceable binding can be measured. The main incubation took either 60 or 90 min and meanwhile slices were light-protected.

For stopping the binding reaction and elimination of remaining ligands and buffer salts, the main incubation is followed by **rinsing** steps in ice-cold buffer solution or ice-cold distilled water, respectively. Finally, slices were dried under a constant stream of air.

Table 1 Binding protocols including the working concentrations of the [^{3}H]ligands and competitors, the incubation steps and buffer compositions. * Chemicals only added to the main incubation.

Receptor	[^{3}H]ligand [concentration in nM]	Competitor [concentration in µM]	Incubation Buffer	Pre-incubation	Main incubation	Rinsing
AMPA	AMPA [9.62]	Quisqualate [10]	50 mM Tris-acetate (pH 7.2) + 100 mM KSCN*	3x 10 min, 4°C	45 min, 4°C	4x 4 sec in buffer, 4°C; 2x 2 sec in 2.5 % Glutaraldehyde in acetone
Kainate	Kainate [9,41]	SYM2081 [100]	50 mM Tris-citrate (pH 7.1) + 10 mM Ca-acetate x H_2O*	3x 10 min, 4°C	45 min, 4°C	3x 4 sec in buffer, 4°C; 2x 2 sec in 2.5 % Glutaraldehyde in acetone
NMDA	MK801 [3.58]	(+)MK801 [100]	50 mM Tris-HCl (pH 7.2) + 50 µM Glutamate + 50 µM Spermidine* + 30 µM Glycine*	15 min, 4°C	60 min, 22°C	2x 5 min in buffer, 4°C; 1 sec in distilled water
mGlu$_{2/3}$	LY341,495 [1.01]	L-Glutamate [1000]	1x PBS (pH 7.4) +137 mM NaCl + 2,7 mM KCl + 4,3 mM Na_2HPO_4 x 2 H_2O + 1,4 mM KH_2PO_4 + 100 mM KBr*	2x 5 min, 22°C	60 min, 4°C	2x 5 min in buffer, 4°C; 1 sec in distilled water
GABA$_A$	Muscimol [7.42]	GABA [10]	50 mM Tris-citrate (pH 7.0)	3x 5 min, 4°C	40 min, 4°C	3x 3 sec in buffer, 4°C; 1 sec in distilled water

BZ	Flumazenil [1.07]	Clonazepam [2]	170 mM Tris-HCl (pH 7.4)	15 min, 4°C	60 min, 4°C	2x 1 min in buffer, 4°C; 1 sec in distilled water
$GABA_B$	CGP54626 [2.11]	CGP55845 [100]	50 mM Tris-HCl (pH 7.2) + 2.5 mM $CaCl_2$ x 2 H_2O	3x 5 min, 4°C	60 min, 4°C	3x 2 sec in buffer, 4°C; 1 sec in distilled water
$D_{2/3}$	Fallypride [3.82]	Haloperidol [10]	50 mM Tris-HCl (pH 7.4) + 120 mM NaCl + 5 mM KCl	30 min, 22°C	60 min, 37°C	2x 2 min, 4°C; 1 sec in distilled water

3.4. Film exposition and development

Radiolabeled brain slices and calibrated plastic standards with increasing concentrations of radioactivity were co-exposed. After drying, slices were fixed on white paper sheets using double-sided adhesive tape, and tritium-sensitive film sheets (Carestream Biomax MR-1, 24x30 cm, Sigma-Aldrich Chemie GmbH, Steinheim, Germany) were placed on top of both. Film sheets and slices were fastened between two plastic plates, to prevent slipping during the exposition, and finally stored into light-protected wooden boxes for ligand-depended exposition times between 9 and 15 weeks (table 2).

Table 2 Film exposition times of the [^{3}H]ligands examined in weeks.

[^{3}H]ligand	**Exposition time [weeks]**
AMPA	15
Kainate	12
MK 801	12
LY341,495	10
Muscimol	12
Flumazenil	9
CGP54626	10
Fallypride	15

After exposition, the film sheets were photographically developed in total darkness by using a tritium-sensitive emulsion (GBX-Developer & DBX-Fixer, Carestream Dental, Atlanta, USA) and a Hyperprocessor (Amersham Biosciences Europe GmbH, Freiburg im Breisgau, Germany).

3.5. Digitalization and densitometric analysis

The exposed film sheets were digitized using the digital camera AxioCam HRc (Carl Zeiss Mikro Imaging GmbH, Germany) connected to the AxioVision Rel. 4.8. Software (Carl Zeiss, Göttingen, Germany). The camera was pre-warmed for 20 min before starting, and the whole digitalization procedure was done in darkness on a homogenous illuminated light table. First, a shading correction was carried out to obtain a homogenous light intensity in the measuring area of the film sheets. Afterwards, the gray value of a homogenous illuminated area of each digitized film-sheet was measured. The resulting brightness was adjusted to a defined range and controlled for every film-sheet. Preparatory settings were not varied during the process of digitalization to guarantee comparable and reproducible images.

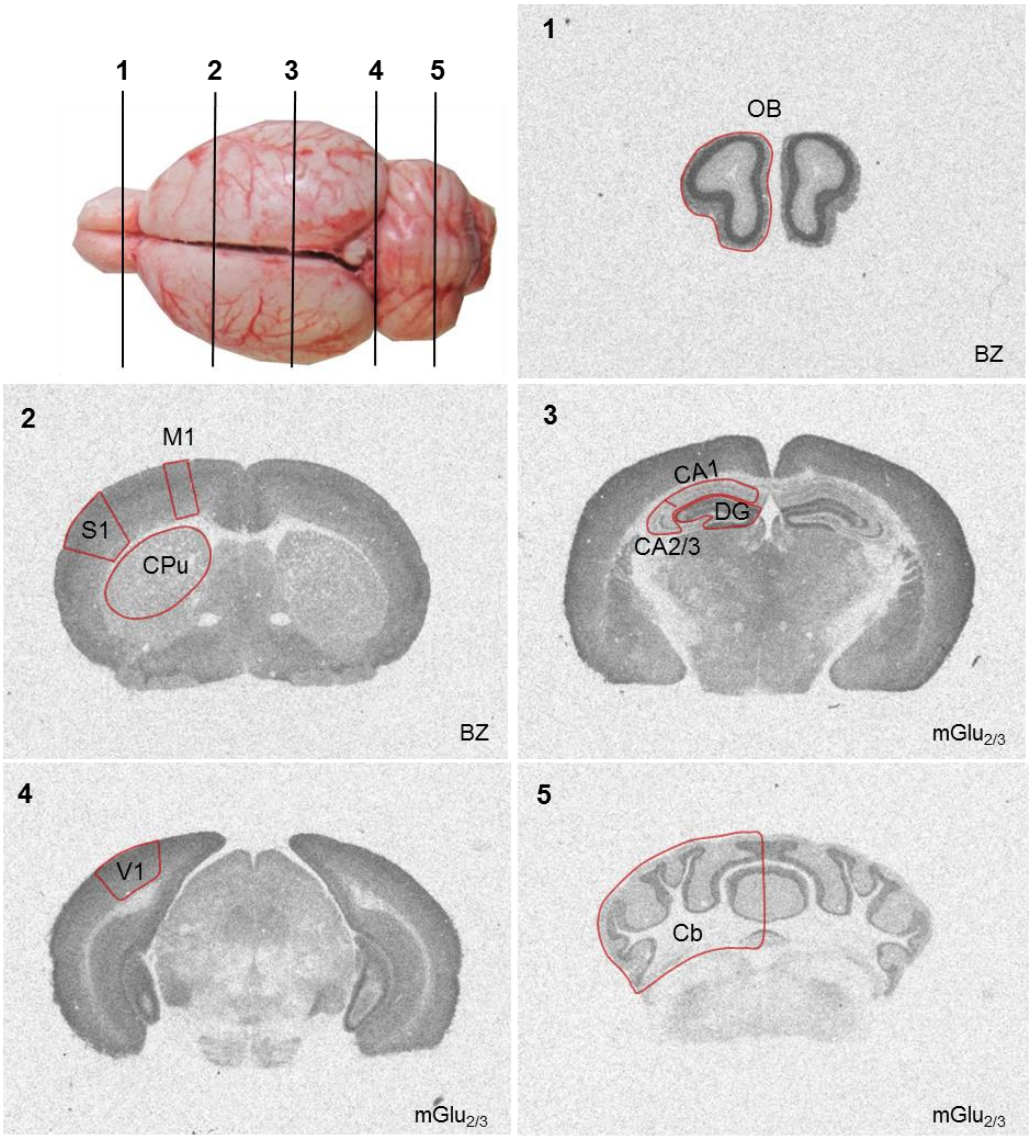

Figure 1 Mouse brain coronal slices showing $GABA_A$ associated benzodiazepine binding sites ([^{3}H]flumazenil) and mGlu2/3 receptors ([^{3}H]LY341,495). Red circled brain regions: (**1**) olfactory bulb (OB); (**2**) striatum (CPu), motor (M1) and somatosensory (S1) cortex; (**3**) hippocampal CA1, CA2/3, DG; (**4**) visual cortex (V1); (**5**) cerebellum (Cb).

The autoradiograms were analyzed using the software AxioVision Rel. 4.8 (Zeiss, Carl Zeiss Mikro Imaging GmbH, Germany) (Palacios et al., 1981; Quirion et al., 1981) and the brain regions were delineated (see figure 1) in both hemispheres based on `The Mouse Brain in Stereotaxic Coordinates´ (Paxinos and Franklin, 2001). Examined brain regions included the olfactory bulb (OB), the motor (M1) and the somatosensory cortex (S1), the striatum (caudate putamen, CPu), the hippocampus including CA (cornu ammonis) 1 and

CA2/3, and DG (dentate gyrus), as well as the visual cortex (V1) and the cerebellum (Cb). For the densitometric measurement, three autoradiograms per mouse brain and investigated region were averaged.

3.6. Calibration, color coding and data analysis

For calibration purposes, co-exposed standards with known concentrations of radioactivity were used to compute non-linear transformation curves. Based on these transformation curves, the gray values of each pixel of an autoradiographic image were converted into concentration of radioactivity and corresponding receptor densities in fmol/ mg protein. The linearized relationship between gray values and receptor densities allowed color-coding of the gray values to visualize specific receptor distributions. Red-colored pixels correspond to high receptor densities (fmol/ mg protein) and low receptor densities were colored in dark blue (figure 2).

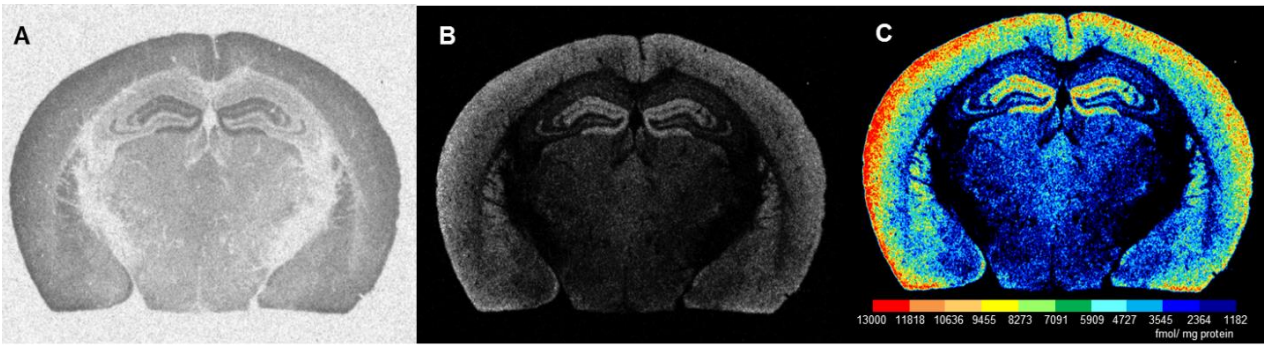

Figure 2 Procedure of color-coding after binding of $mGlu_{2/3}$ receptors with [^{3}H]LY341,495 (**A**) Digitized autoradiogram, (**B**) inverted image for densitometric evaluation and (**C**) converted color-coded image.

3.7. Histological staining

Brain slices were stained using cresyl violet, in accordance with established protocols, to enable the cytoarchitectonic identification of the regions. Alternating slices were formaldehyde fixated and stained using a 0.1 % cresyl violet acetate solution. In order to achieve an optimal staining result, the brain slices were differentiated using 70 % isopropanol. Afterwards, the slices were dehydrated in alcohol solutions of serially

ascending concentrations and finally covered using DPX (dibutylphthalate polystyrene xylene).

3.8. Statistical analysis

We first tested for interhemispheric differences in receptor densities. Global differences for a given receptor type were statistically determined for each region individually by means of an ANOVA (Systat® Version 13) with repeated measures. Bonferroni corrections were applied and threshold was set at $p \leq 0.05$. Since the results of these tests were not significant, data obtained from the left and right hemispheres were pooled for further analyses, and mean and standard deviation of receptor densities were calculated.

Densities of AMPA, kainate, NMDA, $mGlu_{2/3}$, $GABA_A$, and $GABA_B$ receptors were tested separately for statistically significant differences between *Crybb2*^{O377} and wild type mice using an ANOVA (Systat® Version 13) with repeated measures in which the animal groups was treated as a between factor and region as within factor.

Since $D_{2/3}$ receptor densities were below the detection level of in vitro receptor autoradiography in all brain regions but the putamen, we applied an ANOVA with animal groups as a between factor. Bonferroni corrections were applied and threshold was set at $p \leq 0.05$. In the case of a significant result of the Omnibus test, pairwise comparisons would be carried out for the receptor type in question by means of univariate f-tests.

In case of the visual cortex, receptor densities were analyzed by a MANOVA (Systat® Version 13). The statistical analyses was applied with animal groups as independent factor and neurotransmitter system as dependent factors. Bonferroni corrections were applied and threshold was set at $p \leq 0.05$.

4 Results

The receptor densities and distribution patterns of GABAergic ($GABA_A$, BZ, $GABA_B$), glutamatergic (AMPA, kainate, NMDA, and $mGlu_{2/3}$) and dopaminergic ($D_{2/3}$) neurotransmitter receptors were investigated in brains of *Crybb2*^{O377} mice and corresponding control animals, by means of quantitative *in vitro* receptor autoradiography.

The results were tested for statistically significant differences of respective neurotransmitter receptor densities. The statistical analysis indicated no significant changes of neurotransmitter receptor densities in brains of *Crybb2*^{O377}, compared to wild type mice. However, results indicated differential tendencies of altered kainate, $GABA_A$ and $GABA_B$ receptor densities in cataract-affected mice. Tendencies were defined by nominally significant results, which could not be proven to be robust on a correction for multiple comparisons.

4.1. Glutamate receptors

AMPA receptors

No significant differences in AMPA receptor densities could be observed in the examined brain regions of *Crybb2*^{O377} compared to control mice. The color-coded images in figure 4 show the regional distribution pattern of AMPA receptor densities, which was similar in the wild type and *Crybb2*^{O377} mice. AMPA receptor densities were low in the olfactory bulb, the cortical areas M1, S1 and V1 as well as the striatum and the cerebellum. The hippocampal regions CA1, CA2/3 and dentate gyrus exhibited higher AMPA receptor densities.

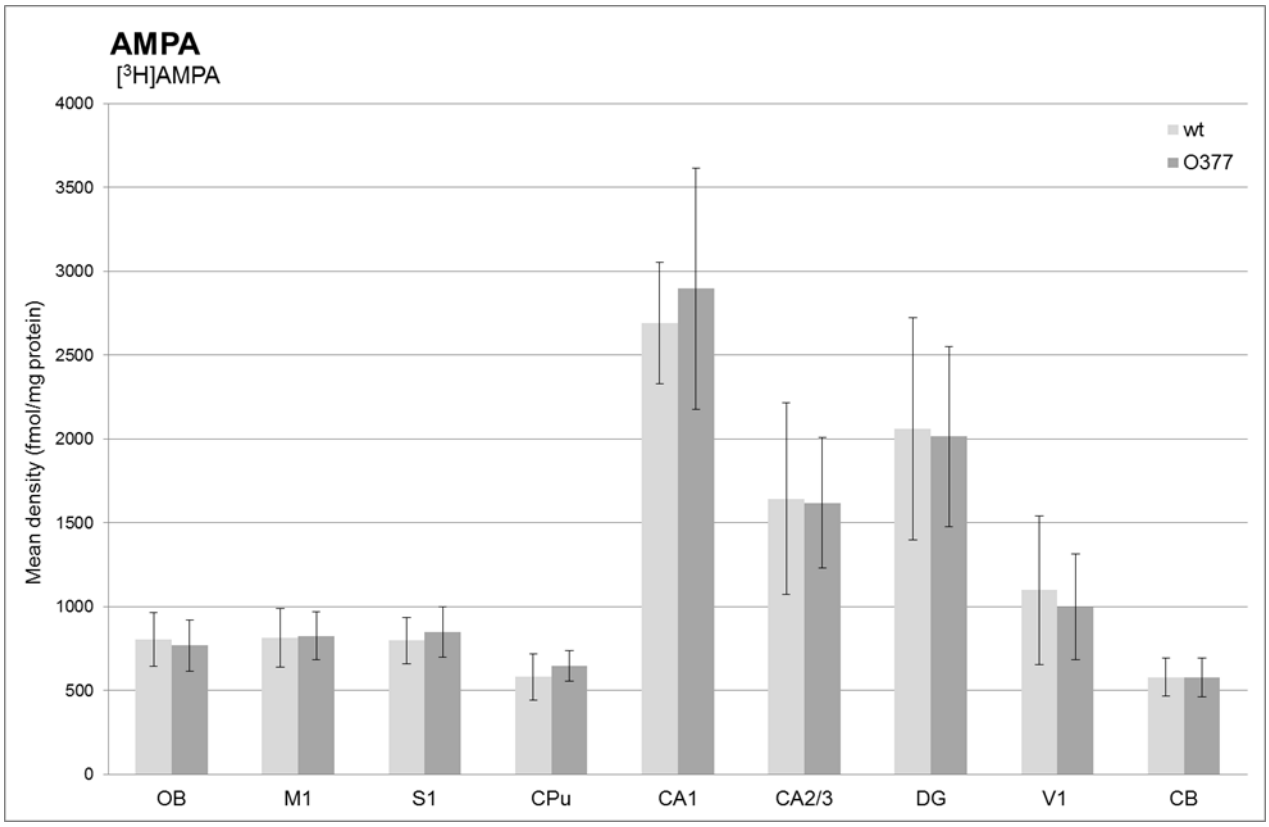

Figure 3 Bar charts showing mean densities (fmol/ mg protein) of AMPA receptors including standard deviation in nine brain regions (OB, M1, S1, CPu, CA1, CA2/3, DG, V1 and Cb) of *Crybb2*^{O377} (O377; n = 10) and corresponding wild type mice (wt; n = 9).

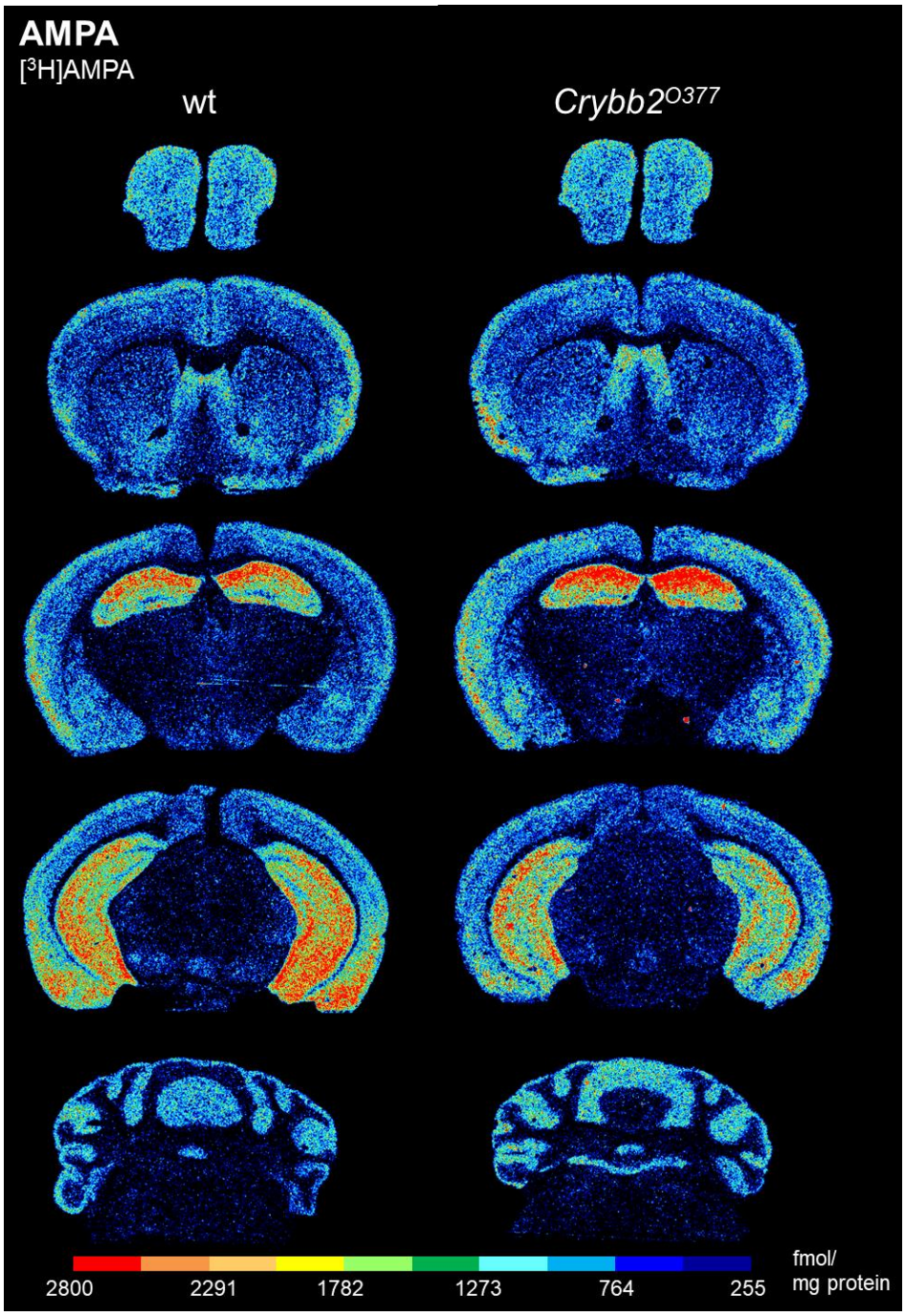

Figure 4 Color-coded images representing the distribution pattern of AMPA receptors in *Crybb2*^{O377} and corresponding wild type mice (wt).

Kainate receptors

No significant differences of kainate receptor densities were determined between the *Crybb2*^{O377} and corresponding wild type mice. However, a tendency towards

downregulated kainate receptor densities could be observed in the visual cortex ($p_{uc} \leq 0{,}01$) of *Crybb2*^{O377} mice. This nominally significant result could not be proven to robust based on a correction for multiple comparisons. Regional distribution patterns of kainate receptors densities were similar between *Crybb2*^{O377} and corresponding wild type mice (see figure 4). The lowest kainate receptor densities were found in the hippocampal CA1 region as well as the cerebellum and the highest in the olfactory bulb. In the other brain regions analyzed kainate receptors were homogeneously distributed.

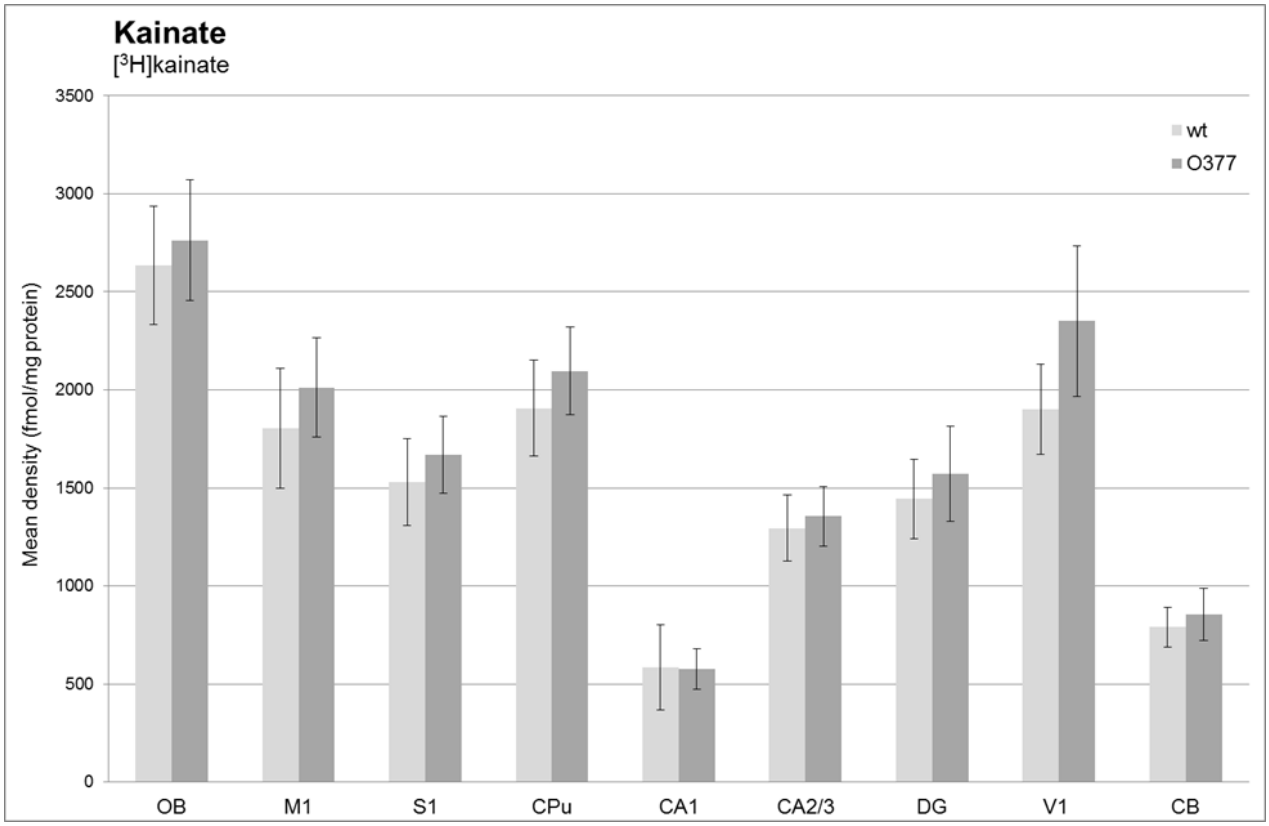

Figure 5 Bar charts showing mean densities (fmol/ mg protein) of kainate receptors including standard deviation in nine brain regions (OB, M1, S1, CPu, CA1, CA2/3, DG, V1 and Cb) of *Crybb2*^{O377} (O377; n = 10) and corresponding wild type mice (wt; n = 9).

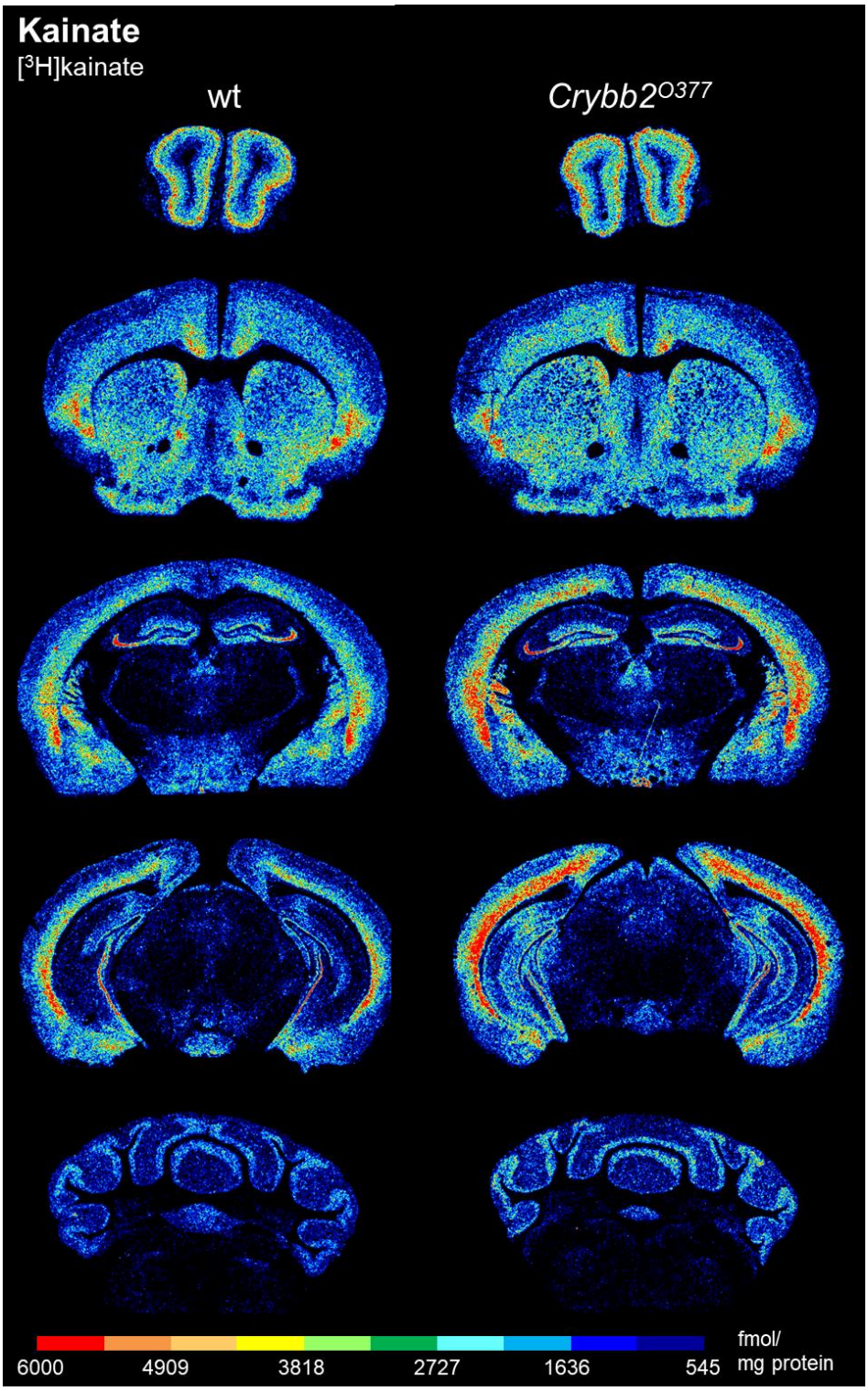

Figure 6 Color-coded images representing the distribution patterns of kainate receptors in *Crybb2*^{O377} and corresponding wild type mice (wt).

NMDA receptors

[^{3}H]MK801 specific NMDA receptors were investigated in all brain regions expect for the cerebellum, where receptor densities were below the detection limit. No significant alterations of NMDA receptor densities could be observed in the brains of *Crybb2^{O377}* mice compared to controls. Figure 8 visualizes NMDA receptor densities, which were similar distributed in the investigated brain regions of *Crybb2^{O377}* and wild type mice. Mean densities of NMDA receptors were similar between most analyzed brain regions, except for the CA1 region and the DG of the hippocampus, where receptor densities were relatively high.

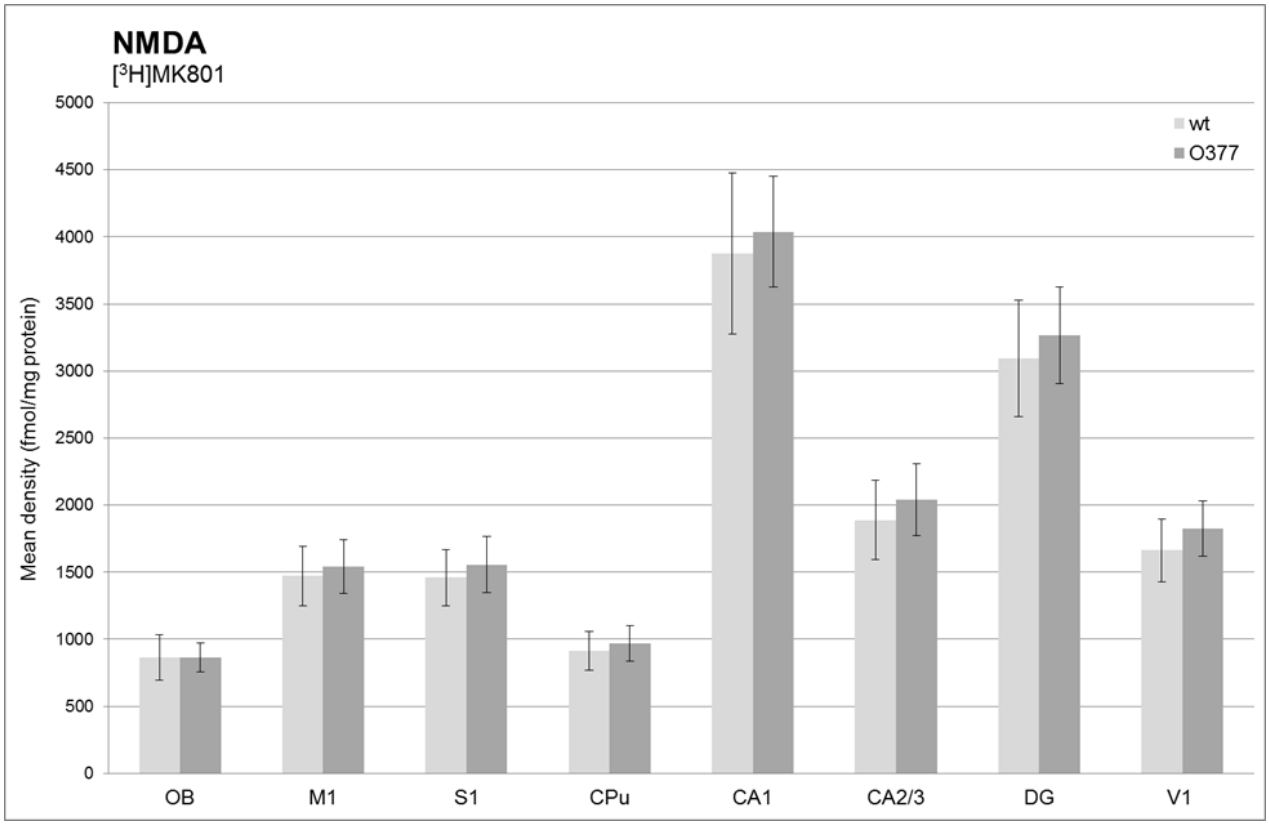

Figure 7 Bar charts showing mean densities (fmol/ mg protein) of NMDA receptors including standard deviation in eight brain regions (OB, M1, S1, CPu, CA1, CA2/3, DG and V1) of *Crybb2^{O377}* (O377; n = 10) and corresponding wild type mice (wt; n = 9).

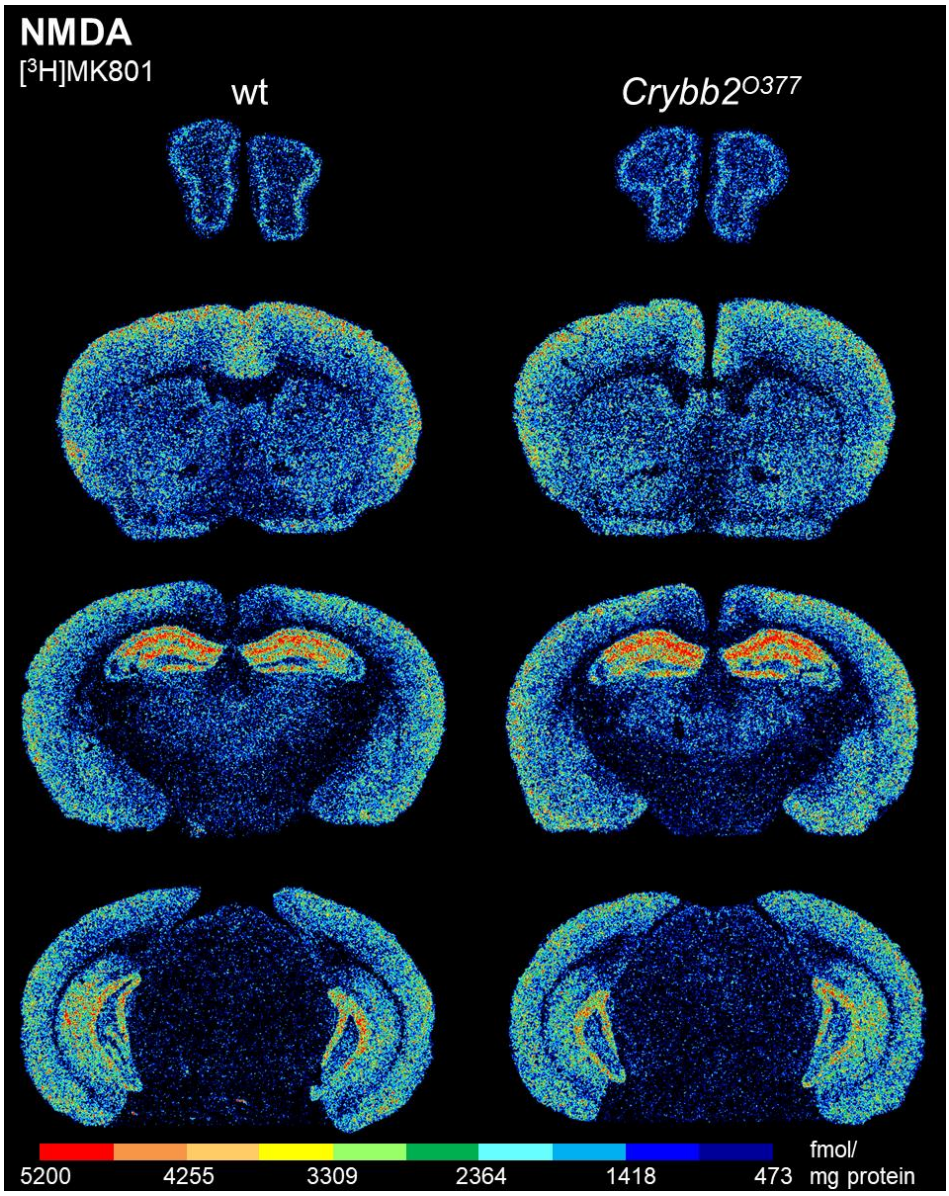

Figure 8 Color-coded images representing the distribution patterns of NMDA receptors in *Crybb2^{O377}* and corresponding wild type mice (wt).

mGlu$_{2/3}$ receptors

No significant metabotropic Glu$_{2/3}$ receptor binding sites could be observed in brains of *Crybb2^{O377}* mice compared to corresponding controls. In general, densities of mGlu$_{2/3}$ receptors are distributed similarly between the investigated brain regions in both animal groups (see figure 8). Low mean receptor densities could be found in the hippocampal

CA1 and CA2/3 regions, as well as the cerebellum. High densities were observed in the cortical areas M1, S1, V1 and the dentate gyrus.

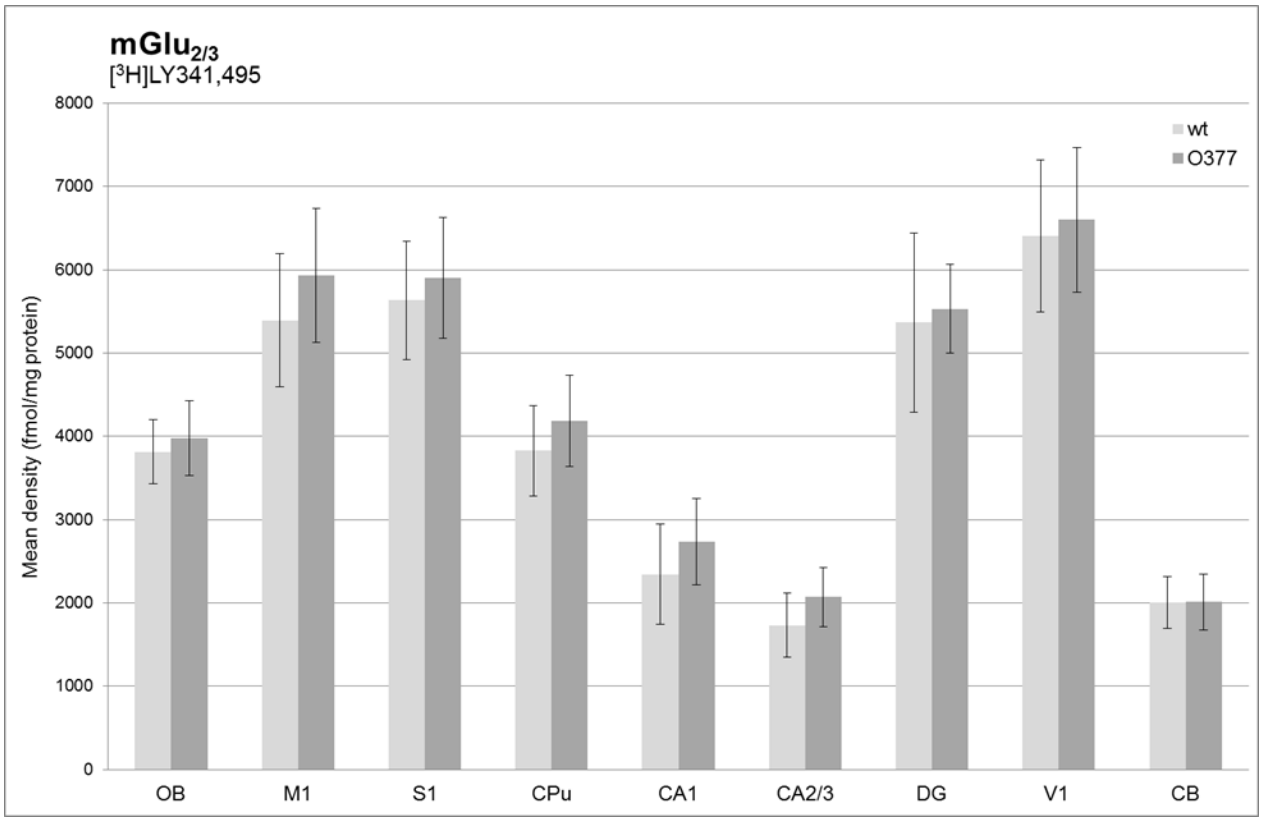

Figure 9 Bar charts showing mean densities (fmol/ mg protein) of $mGlu_{2/3}$ receptors including standard deviation in nine brain regions (OB, M1, S1, CPu, CA1, CA2/3, DG, V1 and Cb) of *Crybb2*^{O377} (O377; n = 10) and corresponding wild type mice (wt; n = 9).

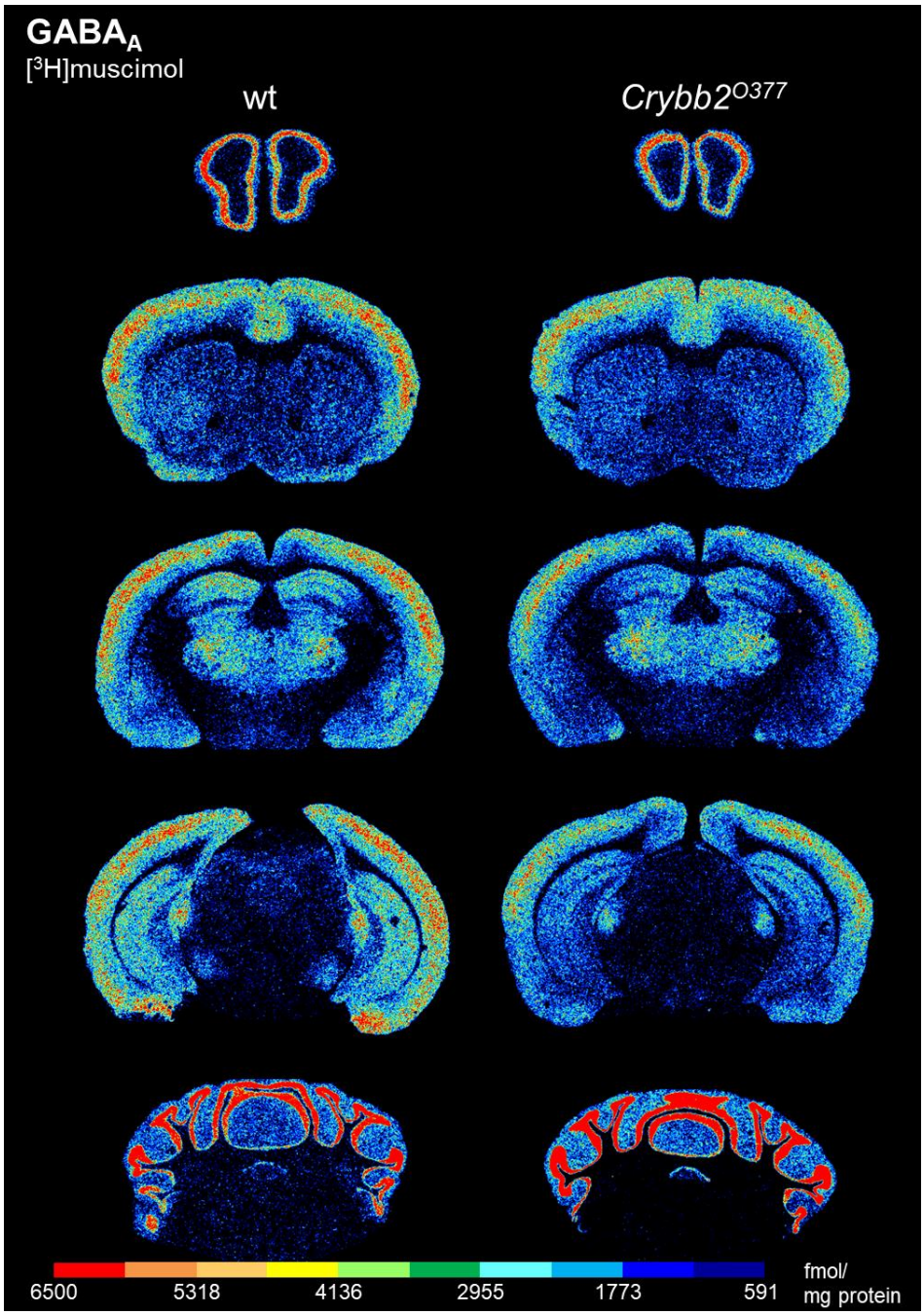

Figure 10 Color-coded images representing the distribution patterns of mGlu$_{2/3}$ receptors in *Crybb2*^{O377} and corresponding wild type mice (wt).

4.2. GABA receptors

$GABA_A$ receptors

No significant differences of $GABA_A$ receptor binding sites could be observed between *Crybb2*^{O377} and wild type mice using [^{3}H]muscimol. However, nominally significant p-values show a tendency of decreased $GABA_A$ receptor densities in the olfactory bulb ($p_{uc} \leq 0{,}05$), the somatosensory cortex ($p_{uc} \leq 0{,}05$) and the hippocampal CA1 region ($p_{uc} \leq 0{,}05$) in *Crybb2*^{O377} mice compared to corresponding controls. These nominally significant results could not be proven to robust based on a correction for multiple comparisons. Regional distribution patterns of $GABA_A$ receptor densities are similar between *Crybb2*^{O377} and control mice. Figure 10 indicates the highest $GABA_A$ receptor densities in the cerebellum and a homogeneous distribution in the other brain regions, expect for the striatum and the CA2/3 region of the hippocampus which exhibited lower densities.

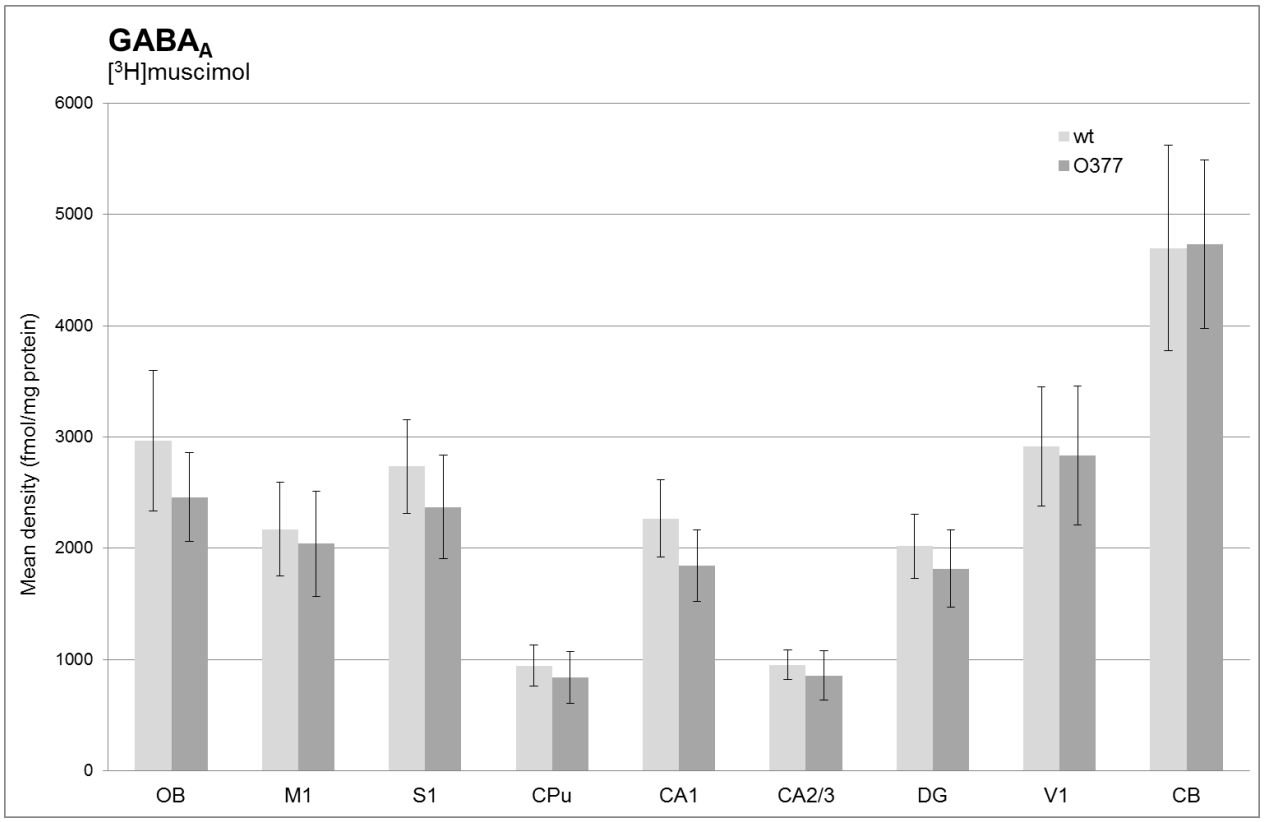

Figure 11 Bar charts showing mean densities (fmol/ mg protein) of $GABA_A$ receptors including standard deviation in nine brain regions (OB, M1, S1, CPu, CA1, CA2/3, DG, V1 and Cb) of *Crybb2*^{O377} (O377; n = 10) and corresponding wild type mice (wt; n = 9).

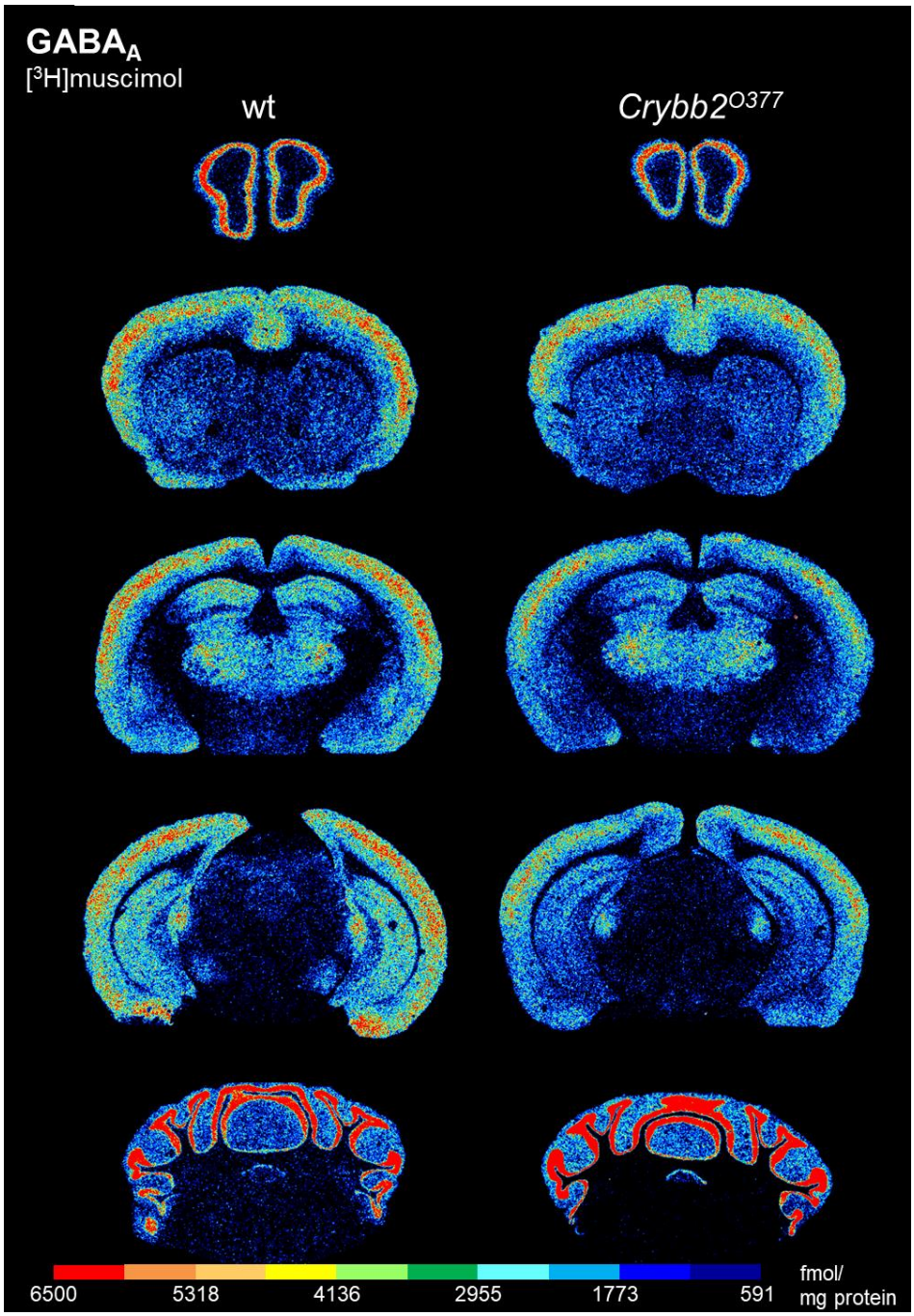

Figure 12 Color-coded images representing distribution patterns of $GABA_A$ receptors in *Crybb2*^{O377} and corresponding wild type mice (wt).

$GABA_A$ associated benzodiazepine binding sites

BZ binding sites were investigated by means of [^{3}H]flumazenil and no significant differences could be found between *Crybb2^{O377}* mice and corresponding control animals. The regional distribution patterns of BZ binding sites were alike between mutated *Crybb2^{O377}* mice and controls. The low densities of $GABA_A$ associated BZ binding sites could be observed in the striatum and the cerebellum. In the other brain regions, analyzed BZ binding site densities were Crybb2ogeneously distributed with slithly higher densities in the olfactory bulb and lower ones in the CA2/3 region of the hippocampus.

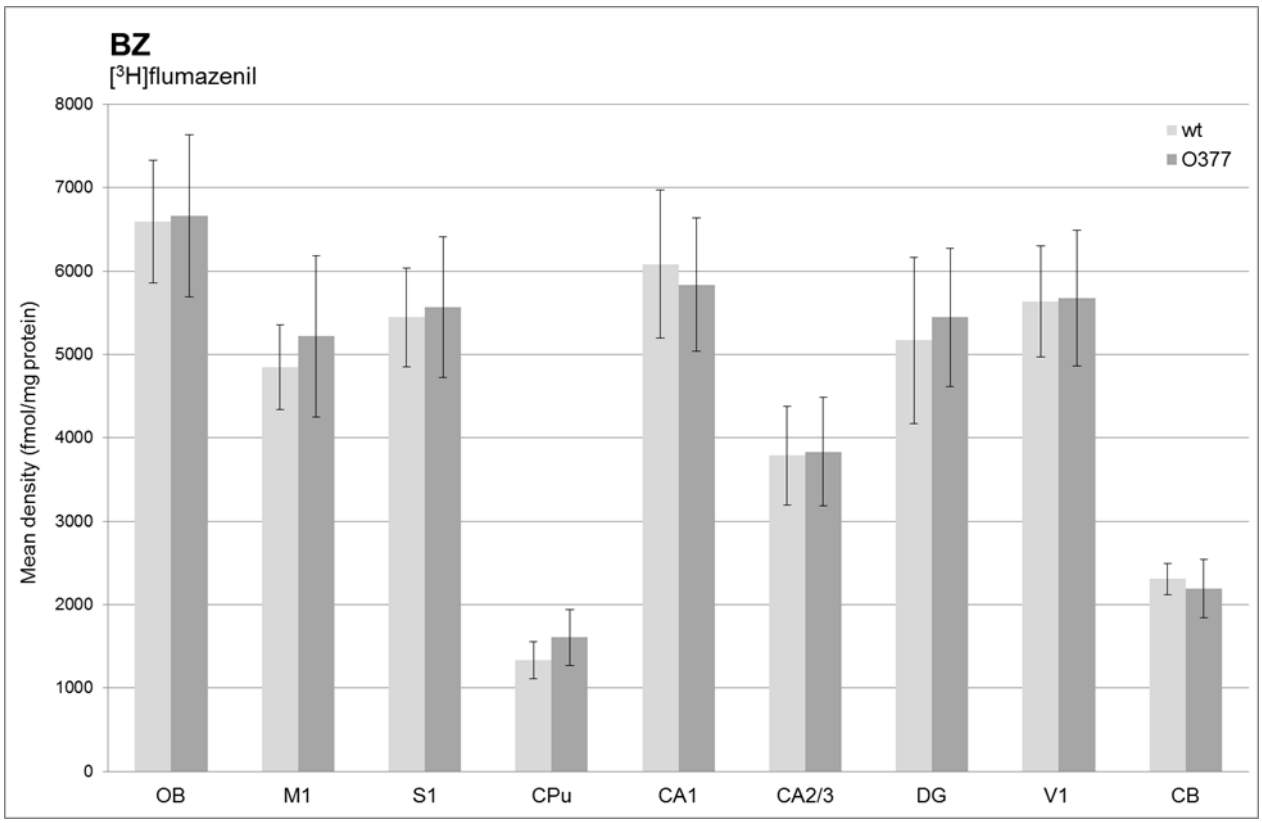

Figure 13 Bar charts showing mean densities (fmol/ mg protein) of benzodiazepine binding sites including standard deviation in nine brain regions (OB, M1, S1, CPu, CA1, CA2/3, DG, V1 and Cb) of *Crybb2^{O377}* (O377; n = 10) and corresponding wild type mice (wt; n = 9).

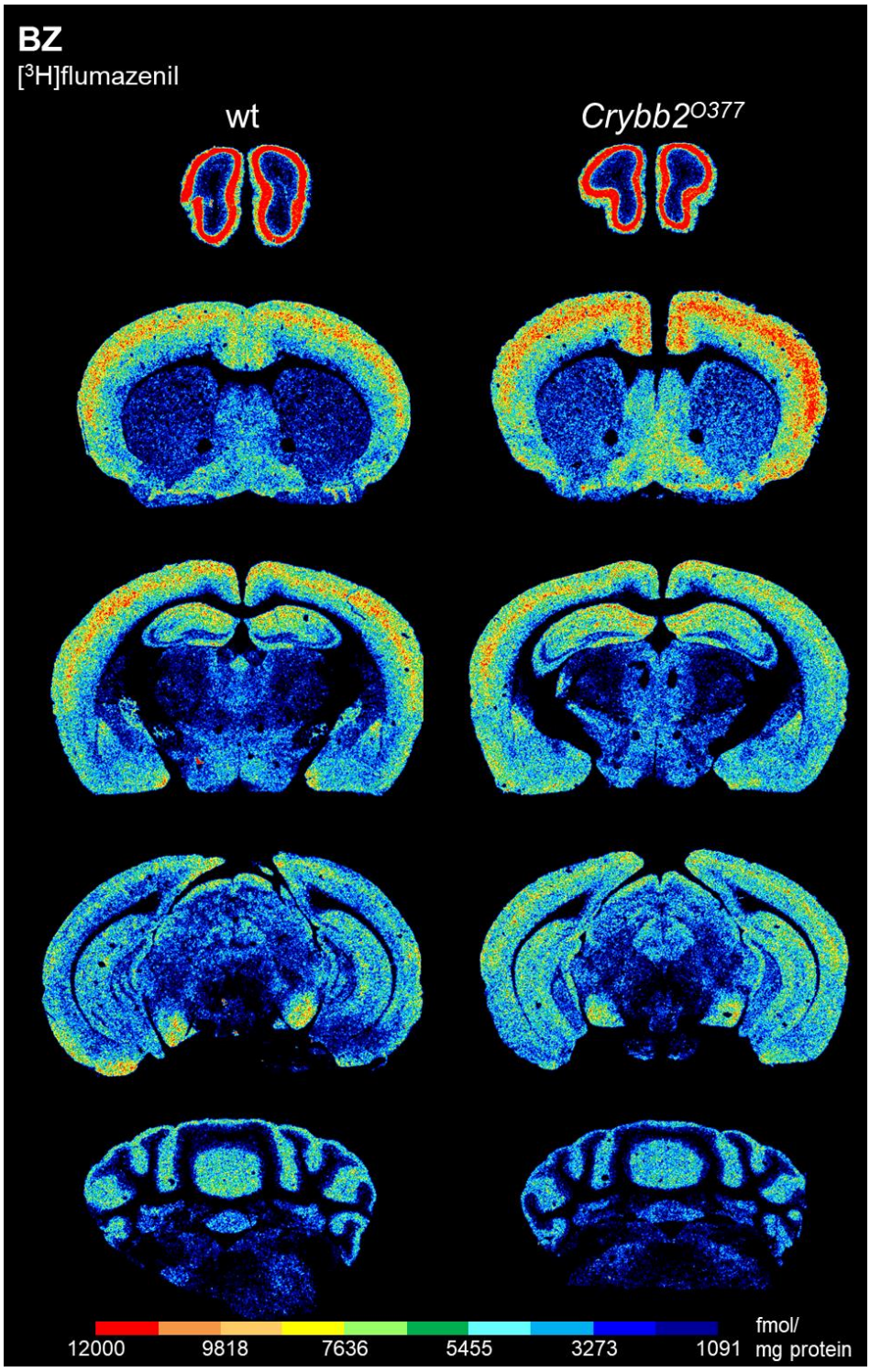

Figure 14 Color-coded images representing the distribution patterns of benzodiazepine binding sites in *Crybb2*^{O377} and corresponding wild type mice (wt).

$GABA_B$ receptors

[^{3}H]CGP54626 specific $GABA_B$ receptor binding sites did not differ significantly between the two experimental animal groups. However, a nominally significant trend towards increased $GABA_B$ receptor binding sites could be observed in the visual cortex ($p_{uc} \leq 0,05$) of *Crybb2^{O377}* mice compared to corresponding controls. These nominal significant result could not be proven to be robust based on a correction for multiple comparisons. Mean densities of $GABA_B$ receptors were comparatively low in the olfactory bulb and the striatum of both groups and homogeneously distributed in the other brain regions examined.

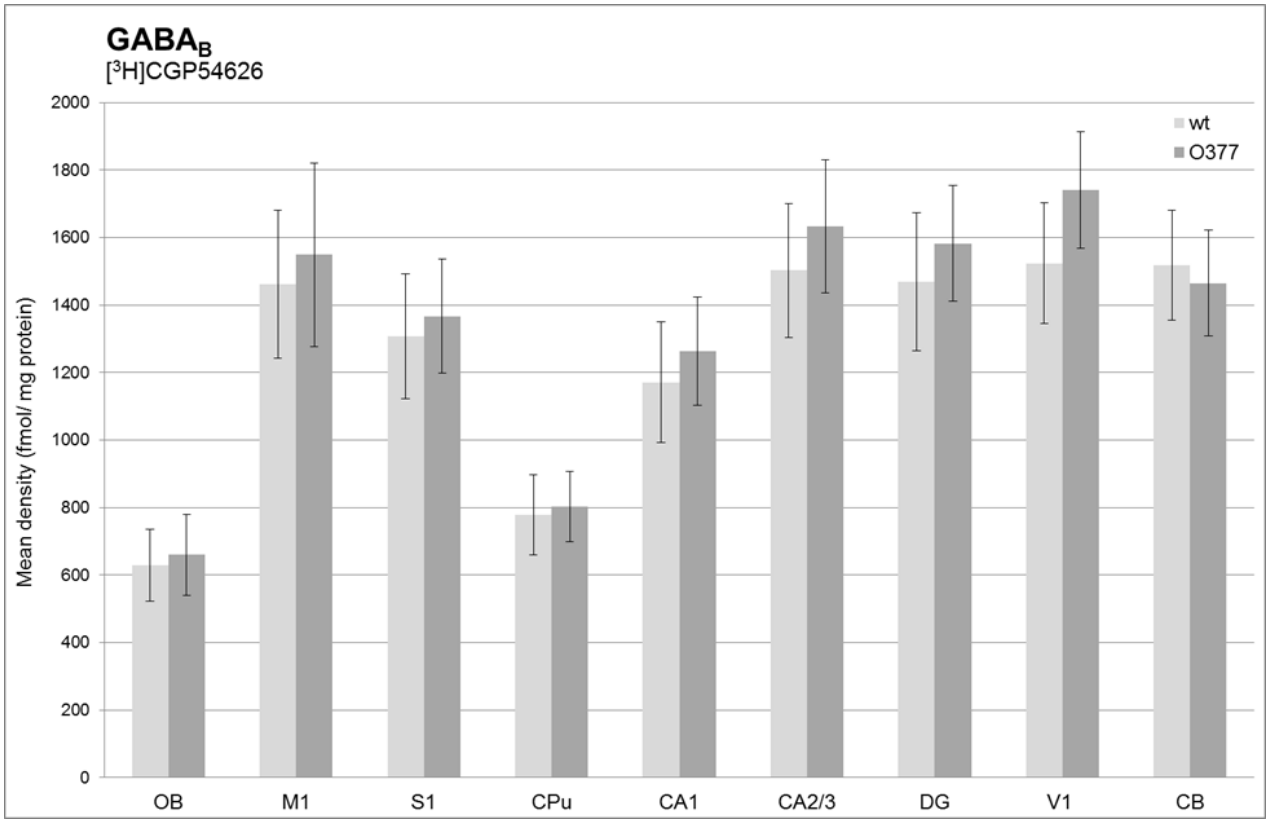

Figure 15 Bar charts showing mean densities (fmol/ mg protein) of $GABA_B$ including standard deviation in nine brain regions (OB, M1, S1, CPu, CA1, CA2/3, DG, V1 and Cb) of *Crybb2^{O377}* (O377; n = 10) and corresponding wild type mice (wt; n = 9).

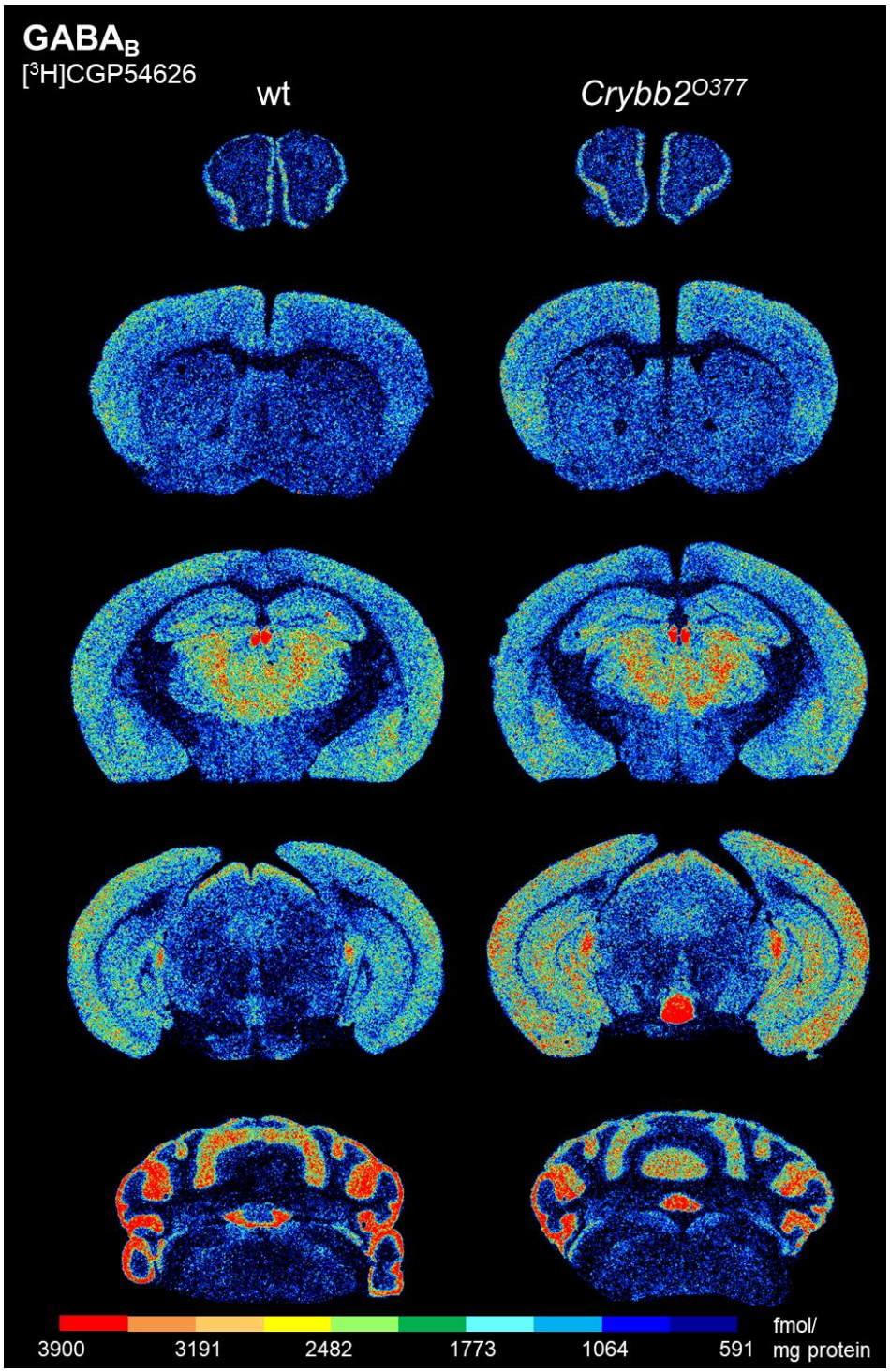

Figure 16 Color-coded images representing the distribution patterns of $GABA_B$ receptors in *Crybb2*^{O377} and corresponding wild type mice (wt).

4.3. Dopamine$_{2/3}$ receptors

$D_{2/3}$ receptors were revealed by [^{3}H]fallypride and analyzed exclusively for the striatum, since the expression level in the other brain regions was below the detection limit. Compared to the wild type, no significant alterations of $D_{2/3}$ receptor binding sites could be found in *Crybb2^{O377}* mice.

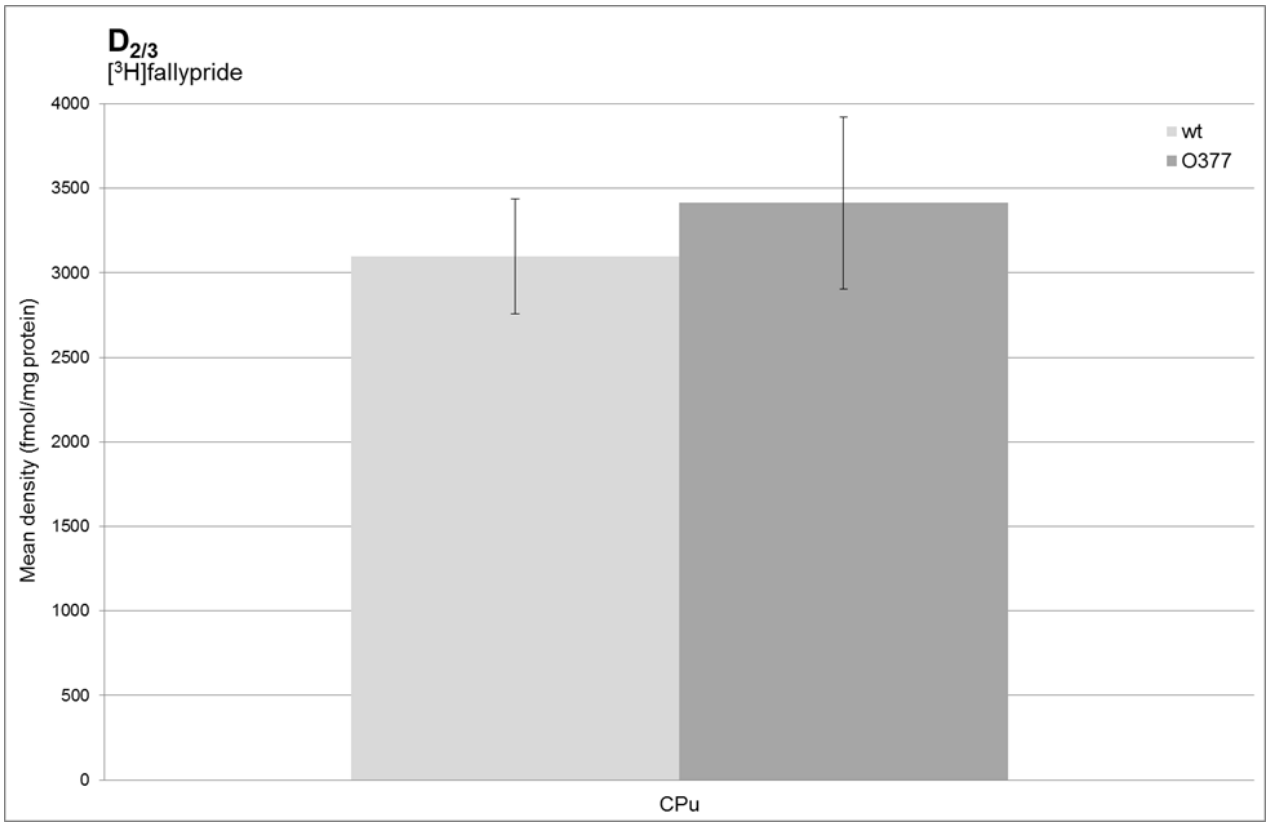

Figure 17 Bar charts showing mean densities (fmol/ mg protein) of $D_{2/3}$ including standard deviation in the striatum (CPu) of *Crybb2^{O377}* (O377; n = 10) and corresponding wild type mice (wt; n = 9).

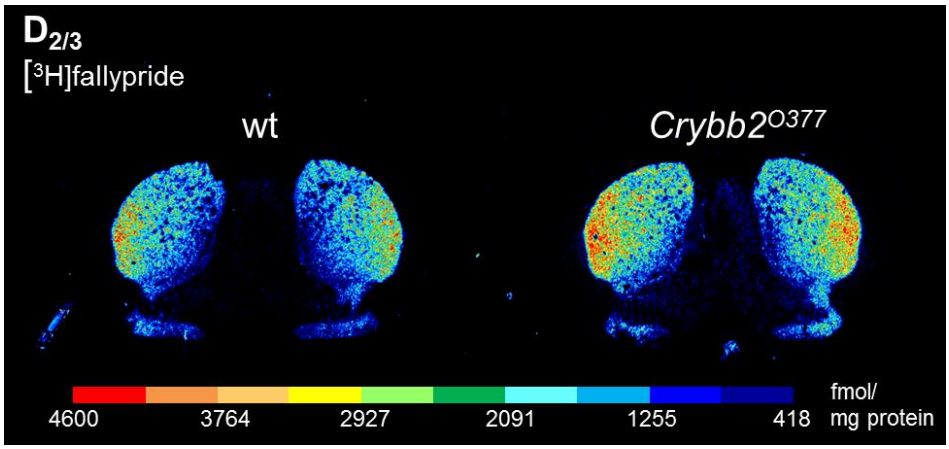

Figure 18 Color-coded images representing the distribution patterns of $D_{2/3}$ receptors in *Crybb2*^{O377} and corresponding wild type mice (wt).

5 Discussion

Age-related cataract is one of the commonest cause of blindness worldwide (Asbell et al., 2005; Song et al., 2014) and the prevalence of cataract development increases with age (Ueda et al., 2002). Extrapolations predicted a continuous increase of cataract patients in the future (Allen Foster, 2000). That points out the importance for obtaining an extensive knowledge of the disease as well as the underlying mechanisms, e.g. via the establishment and comprehensive analysis of corresponding cataract animal models.

In order to obtain a comprehensive overview, quantitative *in vitro* receptor autoradiography was used for the investigation of eight neurotransmitter receptors (glutamatergic: AMPA, kainate, NMDA, $mGlu_{2/3}$; GABAergic: $GABA_A$, BZ, $GABA_B$; dopaminergic: $D_{2/3}$) in the brains of *Crybb2*^{O377} and corresponding control mice. Regarding neurotransmitter receptor densities, no significant alterations between both animal groups could be found. However, differential tendencies of altered kainate, $GABA_A$ and $GABA_B$ receptor densities could be observed in specific brain regions of *Crybb2*^{O377} mice (i.e., olfactory bulb, visual cortex). These nominally significant results could not be proven to be robust based on a correction for multiple comparisons.

5.1. Glutamate receptors

Glutamate is the major excitatory neurotransmitter. In general, glutamate receptors can be subdivided into ionotropic (AMPA, kainate and NMDA) and metabotropic (i.e., $mGlu_{2/3}$) receptors. Under physiological conditions, excitatory neurotransmission plays an important role in mechanisms of synaptic plasticity, e.g. in neurons of the visual system (Kumar et al., 1994). On the other hand, excessive activation of glutamate receptors seems to be involved in neuron damaging, which was described in association to neurological disorders (Choi, 1988; Hollmann and Heinemann, 1994).

In the present study a tendency towards increased **kainate** receptor densities could be observed in the visual cortex of *Crybb2*^{O377} compared to corresponding wild type mice. In general, ionotropic kainate receptors mediate fast excitatory signals to modulate neuronal excitability as well as synaptic plasticity, which underly different cognitive functions, e.g.

in the visual system (Kumar et al., 1994; Morimoto-Tomita et al., 2009; Contractor et al., 2011). A cataract-related trend towards upregulated kainate receptor densities could be an indication for an enhancement of kainate receptor expression rather than changes in receptor affinities. In this case, the visual cortex would have an increased potential for synaptic plasticity mechanisms (Hollmann and Heinemann, 1994; Kumar et al., 1994), potentially being associated to compensatory mechanisms resulting from the visual deficits of *Crybb2*^{O377} mice.

This would be in line with a study from Boroojerdi et al. (2001) which described that visual deprivation induces a rapid increase of neuronal excitability in the visual cortex (Boroojerdi et al., 2001). Therefore, the investigated trend of increased kainate receptors as well as the resulting increased neuronal excitability, could be a mechanism to prevent cognitive decline due to visual deprivation in cataract mice (Maharani et al., 2018). Further investigations are needed to substantiate this thesis.

On the other hand, the trend of upregulated kainate receptors could be an indication for overstimulated glutamate receptor transmission. Under pathological conditions, excessive glutamate receptor activation can lead to excitotoxicity and subsequent neurodegenerative processes (Choi, 1988).

5.2. GABA receptors

The majority of inhibitory signal transmission is mediated through GABA. Its receptors are subdivided into ionotropic $GABA_A$ receptors, including a benzodiazepine binding site and metabotropic $GABA_B$ receptors. Inhibitory GABAergic receptors constitute an important part in the mechanisms of synaptic plasticity in the visual cortex, that are responsible for visual perception and experience during the whole life (Boroojerdi et al., 2001).

In the present study, **$GABA_A$** receptors showed nominally significantly decreased densities in the olfactory bulb, the somatosensory cortex and the hippocampal CA1 region of *Crybb2*^{O377} mice. Inhibitory $GABA_A$ receptors are pentameric assemblies with individual subunit compositions dependent on their brain localization and developmental state (Müller Herde et al., 2017). The high affinity ligand [^{3}H]muscimol binds to all kinds of

$GABA_A$ receptor assemblies (Chandra et al., 2010) and was therefore suitable for the autoradiographic investigation of all $GABA_A$ receptors in the present study.

Under physiological conditions, activation of ionotropic $GABA_A$ receptors opens chloride channels and increases chloride conductance, thus resulting in the inhibition of neuronal firing (Cherubini et al., 1991). As a possible compensatory mechanism, the trend to $GABA_A$ receptor downregulation could counteract increased hyperpolarizing chloride currents, possibly leading to a maintenance of neuronal activity in the brain of *Crybb2*^{O377} mice.

A previous study showed a significant decrease of $GABA_A$ receptors in rats after visual deprivation (He et al., 2006). This is in line with the trend towards downregulated $GABA_A$ receptor densities observed in the present cataract-affected mice.

On the other hand, chloride channels seem to be involved in maintaining lens clarity. In this case, channel disruptions could induce lens opacity consistent with cataract formation (Zhang et al., 1994). Therefore, the tendency towards changed $GABA_A$ receptor densities found in this study could be associated to alterations of chloride currents, which in turn may have negative effects on the lens transparency.

Regarding **$GABA_B$** receptors, nominally significant increased densities could be observed in the visual cortex of *Crybb2*^{O377} mice compared to wild type animals, indicating a possible enhancement of $GABA_B$ receptor expression in the visual cortex of cataract mice. In general, metabotropic $GABA_B$ receptors are involved in processes of synaptic plasticity, e.g. in the visual system (Cartmell and Schoepp, 2000). Thus, the trend towards increased $GABA_B$ receptor densities could be a stimulating process of synaptic plasticity-dependent formation of eye-specific connections (Reid et al., 1996). Furthermore, mechanisms of the synaptic plasticity could counteract the decline of visual function in cataract mice (Lin et al., 2018).

Additionally, $GABA_B$ receptor activations reduces calcium currents due to the inhibition of channel activity (Benke et al., 2012; Turecek et al., 2014). Increased calcium contents may have toxic effects, which seemed to be closely correlated with neuronal degeneration (Choi, 1988). In the case of the present study, the cataract-associated tendency of increased $GABA_B$ receptor densities could have inhibitory effects on cytotoxic calcium currents, thus counteracting possible neurodegenerative processes.

5.3. *Crybb2^{O377}* – A mouse model of cataract

Nominally significant tendencies of differentially altered kainate, $GABA_A$ and $GABA_B$ receptor densities could be observed in specific brain regions (i.e. visual cortex, hippocampal CA1) of *Crybb2^{O377}* mice, but could not be proven to be statistically robust based on a correction for multiple comparisons.
The study was designed using ten *Crybb2^{O377}* and nine wild type mice brains. All mice had the same gender and genetic background in order to ensure low interindividual differences. Nevertheless, a higher sample size might optimize the results and further reduce the standard deviation, thus changing the statistical power of the described results.

The *Crybb2^{O377}* mouse model is based on a mutation in the βB2-crystallin gene (Ganguly et al., 2008). This crystallin subtype constitutes the major lens proteins and seems to be essential for continuous lens clarity by maintaining the water-solubility (Trinkl et al., 1994). Additionally, βB2-crystallins are the least modified proteins during aging, which indicates their essential function (Chen et al., 2013). Thus, we are sure that the *Crybb2^{O377}* mouse is a suitable model for investigations on cataract. However, some optimizing aspects i.e., the age of the *Crybb2^{O377}* mice, are discussed in the following, additional to some approaches for further research.
The nervous system is endowed with potent signaling systems to maintain stable functionality, despite numerous changes during normal development as well as due to neuropathological causes (Kiragasi et al., 2017). The robustness of baseline neurotransmission underscores that changes of neurotransmitter systems mainly occur in a more advanced disease condition (Kiragasi et al., 2017). This could be one reason for the limited detection of changed neurotransmitter receptor densities in the present study.
Comparable to humans, *Crybb2^{O377}* mice show an age-dependent development of the cataract, i.e. in case of the mice, starting postnatal and progressing with age (Graw, 2009). In a *Crybb2* knock out mouse model, the complete opacity of the whole lens was observed after 18 months of age (Zhang et al., 2008). For the present study, brains of 16 to 19 weeks (4-5 months) old *Crybb2^{O377}* mice were used. It could be possible, that the opacity of the mouse lens and subsequent age-related cataract was not completely developed at the time of 4-5 months of age. In this case, the neuronal alterations, e.g. changes in

neurotransmitter receptor densities may also not have been fully developed and therefore only limited detectable. Based on the age-dependency of cataract, nominally higher alterations of neurotransmitter receptor densities, that could be proven to be robust via statistical testing, could probably be determined in older *Crybb2*^{O377} mice (Zhang et al., 2008). Further investigations comparing the present findings with those of older *Crybb2*^{O377} mice as well as with data of age-related cataract in humans would be interesting.

To date, little is known about the behavior of *Crybb2*^{O377} mice. However, a study from Sun et al. (2013) described that *Crybb2*^{O377} mice spend more time with social investigations (Sun et al., 2013). This could indicate a possible compensation for the assumed cataract-dependent visual impairment, via an orientation mode using direct mice clan contact. Mice were also shown to learn and recognize the external environment utilizing non-visual information, i.e., sensory compensation (Iura and Udo, 2014). Based on these results, additional neurotransmitter systems that play an important role for social interaction would be an interesting target for future studies, e.g. the serotonergic system (Olivier et al., 1989; Bibancos et al., 2007).

In general, compensatory mechanisms are an opportunity of the brain to ensure proper functioning of signal transduction in the case of pathological changes, e.g. by dynamic modulation of neuronal synapses. Mechanisms of synaptic plasticity are mainly carried out by neuronal signal mediation i.e., due to glutamatergic and GABAergic transmitter systems (Kumar et al., 1994; Cartmell and Schoepp, 2000). Based on this, it is possible, that neurotransmitter receptors in *Crybb2*^{O377} mice are adjusted with respect to their distribution as well as their densities, thus not exhibiting detectable alterations. In this case again, it would be interesting to analyze older animals to find out, whether changes occur after a certain time point at which the compensatory mechanisms are no longer able to ensure proper functioning. Furthermore, it could be analyzed whether changes in neurotransmitter receptor densities potentially occurring in older mice coincide with behavioral changes or if one effect precedes the other.

6 References

Allen Foster MD, CBM International, Senior Lecturer, Department of Infectious & Tropical Diseases, London School of Hygiene & Tropical Medicine Keppel Street, London WC1, UK (2000) Vision 2020: the cataract challenge. Community Eye Health 13:17-19.

Asbell PA, Dualan I, Mindel J, Brocks D, Ahmad M, Epstein S (2005) Age-related cataract. The Lancet 365:599-609.

Bateman OA, Sarra R, van Genesen ST, Kappé G, Lubsen NH, Slingsby C (2003) The stability of human acidic β-crystallin oligomers and hetero-oligomers. Experimental Eye Research 77:409-422.

Bax B, Lapatto R, Nalini V, Driessen H, Lindley PF, Mahadevan D, Blundell TL, Slingsby C (1990) X-ray analysis of beta B2-crystallin and evolution of oligomeric lens proteins. Nature 347:776-780.

Benke D, Zemoura K, Maier PJ (2012) Modulation of cell surface GABA(B) receptors by desensitization, trafficking and regulated degradation. World journal of biological chemistry 3:61-72.

Bibancos T, Jardim DL, Aneas I, Chiavegatto S (2007) Social isolation and expression of serotonergic neurotransmission-related genes in several brain areas of male mice. Genes, Brain and Behavior 6:529-539.

Boroojerdi B, Battaglia F, Muellbacher W, Cohen LG (2001) Mechanisms underlying rapid experience-dependent plasticity in the human visual cortex. Proceedings of the National Academy of Sciences of the United States of America 98:14698-14701.

Brady JP, Garland D, Duglas-Tabor Y, Robison WG, Groome A, Wawrousek EF (1997) Targeted disruption of the mouse αA-crystallin gene induces cataract and cytoplasmic inclusion bodies containing the small heat shock protein αB-crystallin. Proceedings of the National Academy of Sciences 94:884.

Cancedda L, Fiumelli H, Chen K, Poo M-m (2007) Excitatory GABA Action Is Essential for Morphological Maturation of Cortical Neurons In Vivo. The Journal of Neuroscience 27:5224.

Cartmell J, Schoepp DD (2000) Regulation of neurotransmitter release by metabotropic glutamate receptors. Journal of neurochemistry 75:889-907.

Chalifoux JR, Carter AG (2010) GABAB Receptors Modulate NMDA Receptor Calcium Signals in Dendritic Spines. Neuron 66:101-113.

Chambers C, Russell P (1991) Deletion mutation in an eye lens beta-crystallin. An animal model for inherited cataracts. The Journal of biological chemistry 266:6742-6746.

Chandra D, Halonen LM, Linden A-M, Procaccini C, Hellsten K, Crybb2anics GE, Korpi ER (2010) Prototypic GABA(A) receptor agonist muscimol acts preferentially

through forebrain high-affinity binding sites. Neuropsychopharmacology 35:999-1007.

Chavis P, Shinozaki H, Bockaert J, Fagni L (1994) The metabotropic glutamate receptor types 2/3 inhibit L-type calcium channels via a pertussis toxin-sensitive G-protein in cultured cerebellar granule cells. The Journal of Neuroscience 14:7067.

Chen W, Chen X, Hu Z, Lin H, Zhou F, Luo L, Zhang X, Zhong X, Yang Y, Wu C, Lin Z, Ye S, Liu Y, Study Group of C (2013) A missense mutation in CRYBB2 leads to progressive congenital membranous cataract by impacting the solubility and function of βB2-crystallin. PloS one 8:e81290-e81290.

Chen Y (2014) GABA-A receptor-dependent mechanisms prevent excessive spine elimination during postnatal maturation of the mouse cortex in vivo. FEBS Letters 588:4551-4560.

Cherubini E, Conti F (2001) Generating diversity at GAB Aergic synapses. Trends in Neurosciences 24:155-162.

Cherubini E, Gaiarsa JL, Ben-Ari Y (1991) GABA: an excitatory transmitter in early postnatal life. Trends in Neurosciences 14:515-519.

Choi DW (1988) Glutamate neurotoxicity and diseases of the nervous system. Neuron 1:623-634.

Contractor A, Mulle C, Swanson GT (2011) Kainate receptors coming of age: milestones of two decades of research. Trends in neurosciences 34:154-163.

Corti C, Battaglia G, Molinaro G, Riozzi B, Pittaluga A, Corsi M, Mugnaini M, Nicoletti F, Bruno V (2007) The use of knock-out mice unravels distinct roles for mGlu2 and mGlu3 metabotropic glutamate receptors in mechanisms of neurodegeneration/neuroprotection. The Journal of neuroscience : the official journal of the Society for Neuroscience 27:8297-8308.

Cremer JN, Amunts K, Graw J, Piel M, Rösch F, Zilles K (2015a) Neurotransmitter receptor density changes in Pitx3ak mice – A model relevant to Parkinson's disease. Neuroscience 285:11-23.

Cremer JN, Amunts K, Schleicher A, Palomero-Gallagher N, Piel M, Rosch F, Zilles K (2015b) Changes in the expression of neurotransmitter receptors in Parkin and DJ-1 knockout mice--A quantitative multireceptor study. Neuroscience 311:539-551.

De Filippis B, Lyon L, Taylor A, Lane T, Burnet PWJ, Harrison PJ, Bannerman DM (2015) The role of group II metabotropic glutamate receptors in cognition and anxiety: Comparative studies in GRM2−/−, GRM3−/− and GRM2/3−/− knockout mice. Neuropharmacology 89:19-32.

Ganguly K, Favor J, Neuhauser-Klaus A, Sandulache R, Puk O, Beckers J, Horsch M, Schadler S, Vogt Weisenhorn D, Wurst W, Graw J (2008) Novel allele of crybb2 in the mouse and its expression in the brain. Investigative ophthalmology & visual science 49:1533-1541.

Graw J (2009) Mouse models of cataract. Journal of genetics 88:469-486.

Guyon A, Leresche N (1995) Modulation by different GABAB receptor types of voltage-activated calcium currents in rat thalamocortical neurones. J Physiol 485:29-42.

Hand KS, Baird VH, Van Paesschen W, Koepp MJ, Revesz T, TCrybb2 M, Harkness WF, Duncan JS, Bowery NG (1997) Central benzodiazepine receptor autoradiography in hippocampal sclerosis. Br J Pharmacol 122:358-364.

He H-Y, Hodos W, Quinlan EM (2006) Visual Deprivation Reactivates Rapid Ocular Dominance Plasticity in Adult Visual Cortex. The Journal of Neuroscience 26:2951.

Hollmann M, Heinemann S (1994) Cloned Glutamate Receptors. Annual Review of Neuroscience 17:31-108.

Iura Y, Udo H (2014) Behavioral analyses of visually impaired Crx knockout mice revealed sensory compensation in exploratory activities on elevated platforms. Behavioural Brain Research 258:1-7.

Iversen LL, Mitchell JF, Srinivasan V (1971) The release of γ-aminobutyric acid during inhibition in the cat visual cortex. J Physiol 212:519-534.

Kato AS, Gill MB, Ho MT, Yu H, Tu Y, Siuda ER, Wang H, Qian Y-W, Nisenbaum ES, Tomita S, Bredt DS (2010) Hippocampal AMPA Receptor Gating Controlled by Both TARP and Cornichon Proteins. Neuron 68:1082-1096.

Kiragasi B, Wondolowski J, Li Y, Dickman DK (2017) A Presynaptic Glutamate Receptor Subunit Confers Robustness to Neurotransmission and Crybb2eostatic Potentiation. Cell Reports 19:2694-2706.

Kumar A, Schliebs R, Bigl V (1994) Postnatal development of NMDA, AMPA and kainate receptors in individual layers of rat visual cortex and the effect of monocular deprivation. International Journal of Developmental Neuroscience 12:31-41.

Lampi KJ, Wilmarth PA, Murray MR, David LL (2014) Lens beta-crystallins: the role of deamidation and related modifications in aging and cataract. Progress in biophysics and molecular biology 115:21-31.

Lampi KJ, Ma Z, Hanson SRA, Azuma M, Shih M, Shearer TR, Smith DL, Smith JB, David LL (1998) Age-related Changes in Human Lens Crystallins Identified by Two-dimensional Electrophoresis and Mass Spectrometry. Experimental Eye Research 67:31-43.

Lin H, Zhang L, Lin D, Chen W, Zhu Y, Chen C, Chan KC, Liu Y, Chen W (2018) Visual Restoration after Cataract Surgery Promotes Functional and Structural Brain Recovery. EBioMedicine 30:52-61.

Maharani A, Dawes P, Nazroo J, Tampubolon G, Pendleton N, group SE-CW (2018) Cataract surgery and age-related cognitive decline: A 13-year follow-up of the English Longitudinal Study of Ageing. PloS one 13:e0204833-e0204833.

Moreno MC, de Zavalía N, Sande P, Jaliffa CO, Fernandez DC, Keller Sarmiento MI, Rosenstein RE (2008) Effect of ocular hypertension on retinal GABAergic activity. Neurochemistry international 52:675-682.

Morimoto-Tomita M, Zhang W, Straub C, Cho C-H, Kim KS, Howe JR, Tomita S (2009) Autoinactivation of Neuronal AMPA Receptors via Glutamate-Regulated TARP Interaction. Neuron 61:101-112.

Müller Herde A, Benke D, Ralvenius WT, Mu L, Schibli R, Zeilhofer HU, Krämer SD (2017) GABAA receptor subtypes in the mouse brain: Regional mapping and diazepam receptor occupancy by in vivo [18F]flumazenil PET. NeuroImage 150:279-291.

Nishikawa M, Hirouchi M, Kuriyama K (1997) Functional coupling of Gi subtype with GABAB receptor/adenylyl cyclase system: analysis using a reconstituted system with purified GTP-binding protein from bovine cerebral cortex. Neurochemistry international 31:21-25.

Niswender CM, Conn PJ (2010) Metabotropic glutamate receptors: physiology, pharmacology, and disease. Annu Rev Pharmacol Toxicol 50:295-322.

Nusser Z, Mulvihill E, Streit P, Somogyi P (1994) Subsynaptic segregation of metabotropic and ionotropic glutamate receptors as revealed by immunogold localization. Neuroscience 61:421-427.

Olivier B, Mos J, van der Heyden J, Hartog J (1989) Serotonergic modulation of social interactions in isolated male mice. Psychopharmacology 97:154-156.

Plested AJR, Mayer ML (2007) Structure and Mechanism of Kainate Receptor Modulation by Anions. Neuron 53:829-841.

Reid SNM, Daw NW, Gregory DS, Flavin H (1996) cAMP Levels Increased by Activation of Metabotropic Glutamate Receptors Correlate with Visual Plasticity. The Journal of Neuroscience 16:7619.

Sakurai SY, Cha JH, Penney JB, Young AB (1991) Regional distribution and properties of [3H]MK-801 binding sites determined by quantitative autoradiography in rat brain. Neuroscience 40:533-543.

Scheefhals N, MacGillavry HD (2018) Functional organization of postsynaptic glutamate receptors. Molecular and Cellular Neuroscience 91:82-94.

Scheperjans F, Grefkes C, Palomero-Gallagher N, Schleicher A, Zilles K (2005) Subdivisions of human parietal area 5 revealed by quantitative receptor autoradiography: a parietal region between motor, somatosensory, and cingulate cortical areas. NeuroImage 25:975-992.

Sigel E, Buhr A (1997) The benzodiazepine binding site of GABAA receptors. Trends in Pharmacological Sciences 18:425-429.

Song E, Sun H, Xu Y, Ma Y, Zhu H, Pan C-W (2014) Age-Related Cataract, Cataract Surgery and Subsequent Mortality: A Systematic Review and Meta-Analysis. PloS one 9:e112054.

Sun M, Hölter SM, Stepan J, Garrett L, Genius J, Kremmer E, Hrabě de Angelis M, Wurst W, Lie DC, Bally-Cuif L, Eder M, Rujescu D, Graw J (2013) Crybb2 coding for βB2-crystallin affects sensorimotor gating and hippocampal function. Mamm Genome 24:333-348.

Traynelis SF, Wollmuth LP, McBain CJ, Menniti FS, Vance KM, Ogden KK, Hansen KB, Yuan H, Myers SJ, Dingledine R (2010) Glutamate receptor ion channels: structure, regulation, and function. Pharmacol Rev 62:405-496.

Trinkl S, Glockshuber R, Jaenicke R (1994) Dimerization of beta B2-crystallin: the role of the linker peptide and the N- and C-terminal extensions. Protein Sci 3:1392-1400.

Turecek R, Schwenk J, Fritzius T, Ivankova K, Zolles G, Adelfinger L, Jacquier V, Besseyrias V, Gassmann M, Schulte U, Fakler B, Bettler B (2014) Auxiliary GABAB Receptor Subunits Uncouple G Protein βγ Subunits from Effector Channels to Induce Desensitization. Neuron 82:1032-1044.

Ueda Y, Duncan MK, David LL (2002) Lens Proteomics: The Accumulation of Crystallin Modifications in the Mouse Lens with Age. Investigative ophthalmology & visual science 43:205-215.

Wistow GJ, Piatigorsky J (1988) Lens crystallins: the evolution and expression of proteins for a highly specialized tissue. Annual review of biochemistry 57:479-504.

Zhang J, Li J, Huang C, Xue L, Peng Y, Fu Q, Gao L, Zhang J, Li W (2008) Targeted Knockout of the Mouse βB2-crystallin Gene (Crybb2) Induces Age-Related Cataract. Investigative ophthalmology & visual science 49:5476-5483.

Zhang JJ, Jacob TJ, Valverde MA, Hardy SP, Mintenig GM, Sepúlveda FV, Gill DR, Hyde SC, Trezise AE, Higgins CF (1994) Tamoxifen blocks chloride channels. A possible mechanism for cataract formation. The Journal of Clinical Investigation 94:1690-1697.

Zilles K, Qü MS, Köhling R, Speckmann EJ (1999) Ionotropic glutamate and GABA receptors in human epileptic neocortical tissue: quantitative in vitro receptor autoradiography. Neuroscience 94:1051-1061.

Zilles K, Schleicher A, Palomero-Gallagher N, Amunts K (2002a) 21 - Quantitative Analysis of Cyto- and Receptor Architecture of the Human Brain. In: Brain Mapping: The Methods (Second Edition) (Toga AW, Mazziotta JC, eds), pp 573-602. San Diego: Academic Press.

Zilles K, Schleicher A, Rath M, Glaser T, Traber J (1986) Quantitative autoradiography of transmitter binding sites with an image analyzer. Journal of neuroscience methods 18:207-220.

Zilles K, Palomero-Gallagher N, Grefkes C, Scheperjans F, Boy C, Amunts K, Schleicher A (2002b) Architectonics of the human cerebral cortex and transmitter receptor fingerprints: reconciling functional neuroanatomy and neurochemistry. European Neuropsychopharmacology 12:587-599.

7 Appendix

Chemicals and technical equipment

Preparation of slices:

- Cryostat Leica CM3050 (Leica Biosystems Vertrieb GmbH, Wetzlar, Germany)
- Ethanol (Merck KGaA, Darmstadt, Germany)
- Isopentane (Honeywell GmbH, Seelze, Germany)
- Paraformaldehyde (Sigma-Aldrich Chemie GmbH, Steinheim, Germany)
- Phosphate buffered saline (PBS) (Invitrogen Life Technologies GmbH, Darmstadt, Germany)
- Silan-coated microscope slides (Starfrost, 76x26 mm, Germany)
- Tissue Tec (Sakura Finetek Germany GmbH)

Receptor autoradiography

Buffers and solutions:

- Acetone (VWR International, Langenfeld, Germany)
- Calcium acetate dihydrate (Ca-acetate * H_2O) (Sigma-Aldrich Chemie GmbH, Steinheim, Germany)
- Calcium chloride dihydrate ($CaCl_2$ x 2 H_2O) (VWR International, Langenfeld, Germany)
- Glutaraldehyde (Sigma-Aldrich Chemie GmbH, Steinheim, Germany)
- Glycine (Sigma-Aldrich Chemie GmbH, Steinheim, Germany)
- Glutamate (Sigma-Aldrich Chemie, Steinheim, Germany)
- Potassium bromide (KBr) (VWR International, Langenfeld, Germany)
- Potassium chloride (KCl) (VWR International, Langenfeld, Germany)
- Potassium phosphate monobasic (KH_2PO_4) (VWR International, Langenfeld, Germany)
- Potassium thiocyanate (KSCN) (Sigma-Aldrich Chemie, Steinheim, Germany)
- Sodium chloride (NaCl) (VWR International, Langenfeld, Germany)

- Sodium phosphate dibasic dihydrate (Na_2HPO_4 * 2 H_2O) (Merck KGaA, Darmstadt, Germany)
- Spermidine (Sigma-Aldrich Chemie, Steinheim, Germany)
- Tris-acetate (Sigma-Aldrich Chemie, Steinheim, Germany)
- Tris-citrate (Sigma-Aldrich Chemie, Steinheim, Germany)
- Tris hydrochloride (HCl) (Sigma-Aldrich Chemie, Steinheim, Germany)

[^{3}H]ligands:

- AMPA (PerkinElmer, Rodgau, Germany)
- CGP 54626 (PerkinElmer, Rodgau, Germany)
- Fallypride (Institute of Nuclear Chemistry, Johannes Gutenberg University Mainz, Germany)
- Flumazenil (PerkinElmer, Rodgau, Germany)
- Kainate (PerkinElmer, Rodgau, Germany)
- LY 341,495 (PerkinElmer, Rodgau, Germany)
- MK 801 (PerkinElmer, Rodgau, Germany)
- Muscimol (PerkinElmer, Rodgau, Germany)

Competitors:

- (+)MK 801 (Biotrend Chemikalien GmbH, Cologne, Germany)
- Clonazepam (solution 1mg/ml) (Sigma-Aldrich Chemie, Steinheim, Germany)
- GABA (Biotrend Chemikalien GmbH, Cologne, Germany)
- Haloperidol (Sigma-Aldrich Chemie, Steinheim, Germany)
- L-Glutamic acid (Sigma-Aldrich Chemie, Steinheim, Germany)
- Quisqualate (Biotrend Chemikalien GmbH, Cologne, Germany)
- SYM 2081 (Sigma-Aldrich Chemie, Steinheim, Germany)

Film exposition and development

- GE Healthcare Amersham Hyperfilm (Carestream Biomax MR-1, 24x30 cm, Sigma-Aldrich Chemie GmbH, Steinheim, Germany)
- GBX-Developer (Carestream Dental, Atlanta, USA)
- GBX-Fixer (Carestream Dental, Atlanta, USA)
- Hyperprocessor SRX-101A (Amersham Biosciences Europe GmbH, Freiburg im Breisgau, Germany)

Digital processing

- AxioVision Image Analyzer Rel. 4. 8. (Carl Zeiss Mikroimaging GmbH, Göttingen, Germany)
- Digital camera AxioCam HRc (Carl Zeiss Mikroimaging GmbH, Göttingen, Germany)

Histological staining

- Acetic acid (Merck KGaA, Darmstadt, Germany)
- Cresyl violet (Merck KGaA, Darmstadt, Germany)
- DPX mountant (Fluka, Sigma-Aldrich Chemie GmbH, Steinheim, Germany)
- Formaldehyde solution (Merck KGaA, Darmstadt, Germany)
- 2-Propanol (Merck KGaA, Darmstadt, Germany)
- Sodium acetate (Merck KGaA, Darmstadt, Germany)
- Sodium phosphate dibasic (Merck KGaA, Darmstadt, Germany)
- Sodium phosphate monobasic monohydrate (Merck KGaA, Darmstadt, Germany)
- XEM 200 (DiaTec, Diagnostische Systemtechnik, Bamberg Germany)

8 Raw data

Table 3 Quantitative receptor densities of ampa [fmol/ mg protein] in brain regions of wild type mice (wt) (l=left and r=right hemisphere). Mean ± standard deviation calculated.

AMPA	Animal	11	12	18	22	23	27	28	33	39	Mean ± SD
	Group	wt	wt	wt	wt	wt	wt	wt	wt	wt	
OB	l	754	670	831	580	715	835	1128	935	847	804 ± 161
	r	782	637	733	607	629	873	1126	963	832	
M1	l	794	737	631	643	672	825	982	1142	1069	815 ± 175
	r	810	696	649	597	633	794	960	1048	998	
S1	l	771	752	637	652	680	872	890	1006	1027	798 ± 139
	r	764	767	707	571	654	782	866	939	1021	
CPu	l	504	514	542	462	432	664	659	930	603	582 ± 138
	r	528	518	538	428	449	595	663	873	576	
CA1	l	2209	3212	2466	2883	2602	2822	2653	5719	3085	2694 ± 362
	r	2076	3190	2463	2628	2285	2761	2518	5748	3245	
CA2/3	l	1095	1906	1396	1236	1312	1667	1399	3116	1632	1645 ± 573
	r	1220	1891	1387	1397	1234	1452	1416	3056	1795	
DG	l	1516	2311	1734	1914	1728	1917	1800	3846	2063	2062 ± 664
	r	1416	2304	1658	1763	1588	1922	1728	3641	2274	
V1	l	778	905	883	732	789	1116	1092	2136	1264	1099 ± 443
	r	828	1075	748	659	782	1198	1139	2179	1475	

Cb	**l**	527	603	548	389	421	689	583	694	685	580 ± 112
	r	583	629	616	410	421	708	526	726	689	

Table 4 Quantitative receptor densities of ampa [fmol/ mg protein] in brain regions of *Crybb2* mutants (l=left and r=right hemisphere). Mean ± standard deviation calculated.

AMPA	**Animal**	**1**	**10**	**13**	**29**	**32**	**34**	**36**	**37**	**40**	**41**	**Mean ± SD**
	Group	**Crybb2**	**Crybb2**	**Crybb2**	**Crybb2**	**Crybb2**	**Crybb2**	**Crybb2**	**Crybb2**	**Crybb2**	**Crybb2**	
OB	**l**	792	661	731	652	684	793	755	806	1112	799	768 ± 151
	r	774	542	661	671	655	701	730	775	1181	889	
M1	**l**	995	755	631	743	704	741	889	832	1068	953	826 ± 143
	r	1084	729	671	693	713	739	862	733	1033	956	
S1	**l**	906	661	767	692	764	921	852	778	1113	1071	849 ± 151
	r	962	642	867	661	777	745	891	752	1048	1116	
CPu	**l**	780	555	663	538	640	653	550	604	737	786	648 ± 92
	r	737	538	677	531	633	663	529	609	716	812	
CA1	**l**	2709	1981	2297	1960	2487	2868	3709	3696	3638	4097	2896 ± 720
	r	2496	2046	2894	1639	2548	2840	3894	3296	3374	3459	
CA2/3	**l**	1552	1150	1413	1160	1338	1462	2076	1956	2148	2258	1619 ± 388
	r	1583	1138	1789	858	1525	1420	2127	1760	1798	1879	
DG	**l**	1922	1369	1745	1256	1634	1872	2381	2526	2573	3033	2014 ± 535
	r	1726	1409	2092	1124	1676	1903	2783	2460	2400	2405	
V1	**l**	1142	753	1025	672	986	911	864	1056	1845	959	998 ± 315

	r	1074	688	793	603	989	886	886	1031	1790	1005	
Cb	**l**	542	460	516	492	688	578	740	463	803	622	480 ± 116
	r	535	405	479	449	617	699	616	496	779	620	

Table 5 Quantitative receptor densities of kainate [fmol/ mg protein] in brain regions of wild type mice (wt) (l=left and r=right hemisphere). Mean ± standard deviation calculated.

Kainate	**Animal**	**11**	**12**	**18**	**22**	**23**	**27**	**28**	**33**	**39**	**Mean ± SD**
	Group	**wt**	**wt**	**wt**	**wt**	**wt**	**wt**	**wt**	**wt**	**wt**	
OB	**l**	2803	2916	1931	2527	2527	2819	2498	2717	2467	2634 ± 302
	r	3082	2961	2032	2628	2518	2929	2665	2863	2532	
M1	**l**	1568	2102	1102	1761	1940	2125	2012	1812	1866	1803 ± 305
	r	1672	2000	1083	1682	1811	2184	1970	1866	1896	
S1	**l**	1519	1738	1016	1586	1692	1803	1473	1627	1558	1530 ± 221
	r	1493	1593	1014	1485	1397	1810	1599	1679	1458	
CPu	**l**	1855	2257	1361	2161	2049	2079	1825	2069	1835	1906 ± 244
	r	1812	2133	1354	1987	1883	2106	1861	1923	1760	
CA1	**l**	523	569	324	608	1375	640	528	588	527	585 ± 217
	r	532	558	315	619	602	647	488	574	506	
CA2/3	**l**	1323	1385	943	1499	1373	1594	1264	1236	1264	1295 ± 170
	r	1262	1438	940	1392	1301	1420	1227	1353	1107	
DG	**l**	1483	1613	1017	1562	1384	1673	1440	1518	1316	1444 ± 203
	r	1427	1595	1016	1536	1437	1753	1275	1636	1309	

Raw data

V1	**l**	1732	2249	1595	2030	1886	2269	1777	2196	1810	1900 ± 229
	r	1734	1854	1433	1973	1776	2132	1804	2119	1832	
Cb	**l**	770	663	605	790	930	912	775	877	802	791 ± 101
	r	814	662	650	765	929	897	752	888	756	

Table 6 Quantitative receptor densities of kainate [fmol/ mg protein] in brain regions of *Crybb2* mutants (l=left and r=right hemisphere). Mean ± standard deviation calculated.

Kainate	**Animal**	**1**	**10**	**13**	**29**	**32**	**34**	**36**	**37**	**40**	**41**	**Mean ± SD**
	Group	**Crybb2**	**Crybb2**	**Crybb2**	**Crybb2**	**Crybb2**	**Crybb2**	**Crybb2**	**Crybb2**	**Crybb2**	**Crybb2**	
OB	**l**	2564	2731	2161	2929	2547	3408	2893	2867	2743	2788	2763 ± 309
	r	2562	2771	2146	2683	2591	3351	2923	3010	2764	2835	
M1	**l**	2202	1834	1547	1864	1902	1997	2201	2301	2319	2148	2012 ± 252
	r	2102	1764	1474	1756	1980	1989	2260	2359	2236	2009	
S1	**l**	1834	1665	1246	1659	1617	1641	1754	1743	1904	1715	1667 ± 196
	r	1837	1522	1185	1497	1619	1685	1796	1800	1985	1632	
CPu	**l**	2236	2081	1692	2416	1860	2055	2191	2304	2291	2193	2097 ± 222
	r	2190	1942	1655	2024	1808	2024	2257	2339	2380	2004	
CA1	**l**	625	596	334	543	608	609	601	726	670	485	577 ± 103
	r	621	593	321	535	616	575	627	696	644	513	
CA2/3	**l**	1375	1482	991	1339	1522	1452	1420	1475	1464	1252	1355 ± 153
	r	1248	1464	950	1299	1379	1390	1501	1374	1415	1314	
DG	**l**	1669	1666	1077	1343	1617	1533	1750	1973	1694	1376	

Raw data

	r	1643	1673	1013	1355	1653	1585	1825	1809	1742	1425	1571 ± 242
V1	l	2658	2174	1576	2297	2482	2308	2310	3083	2699	2561	2351 ± 384
	r	2340	2147	1399	2409	2239	2071	2392	2848	2487	2547	
Cb	l	893	909	534	869	785	810	925	1001	918	912	856 ± 133
	r	869	918	503	861	777	807	939	1038	952	891	

Table 7 Quantitative receptor densities of NMDA [fmol/ mg protein] in brain regions of wild type mice (wt) (l=left and r=right hemisphere). Mean ± standard deviation calculated.

NMDA	Animal	11	12	18	22	23	27	28	33	39	Mean ± SD
	Group	wt	wt	wt	wt	wt	wt	wt	wt	wt	
OB	l	897	1204	947	923	786	778	658	877	666	862 ± 170
	r	863	1250	958	930	785	778	650	906	655	
M1	l	1548	1920	1615	1590	1447	1431	1209	1497	1112	1473 ± 222
	r	1481	1805	1506	1580	1442	1355	1245	1668	1067	
S1	l	1517	1910	1520	1601	1390	1445	1182	1547	1180	1461 ± 210
	r	1493	1815	1509	1486	1367	1379	1127	1625	1196	
CPu	l	969	1089	1038	1015	807	892	740	1111	710	913 ± 143
	r	943	1040	941	949	800	893	702	1114	687	
CA1	l	3903	4831	4331	3963	3651	3514	2910	4191	3203	3877 ± 602
	r	4241	5052	4174	3908	3950	3680	2957	4287	3035	
CA2/3	l	1834	2458	2065	1858	1880	1722	1410	1949	1497	

Raw data

	r	1997	2471	1961	1877	1950	1741	1535	2227	1574	1889 ± 197
DG	l	3118	3759	3394	3314	3336	2933	2397	3278	2441	3093 ± 432
	r	3224	3691	3305	3234	3421	2827	2365	3184	2457	
V1	l	1610	2220	1770	1654	1626	1707	1336	1669	1354	166 ± 234
	r	1738	2073	1791	1723	1651	1655	1367	1670	1324	

Table 8 Quantitative receptor densities of NMDA [fmol/ mg protein] in brain regions of *Crybb2* mutants (l=left and r=right hemisphere). Mean ± standard deviation calculated.

NMDA	**Animal**	**1**	**10**	**13**	**29**	**32**	**34**	**36**	**37**	**40**	**41**	**Mean ± SD**
	Group	**Crybb2**	**Crybb2**	**Crybb2**	**Crybb2**	**Crybb2**	**Crybb2**	**Crybb2**	**Crybb2**	**Crybb2**	**Crybb2**	
OB	**l**	974	898	863	962	634	793	850	816	1000	883	864 ± 106
	r	973	879	918	969	628	783	813	803	990	860	
M1	**l**	1834	1461	1814	1660	1179	1415	1393	1523	1843	1635	1543 ± 199
	r	1620	1444	1716	1682	1259	1272	1320	1482	1706	1599	
S1	**l**	1701	1495	1885	1707	1156	1477	1355	1530	1868	1599	1556 ± 208
	r	1590	1502	1712	1753	1118	1451	1374	1472	1785	1587	
CPu	**l**	1024	993	1096	1072	718	834	861	922	1239	979	967 ± 132
	r	989	974	1020	1032	718	898	857	949	1183	981	
CA1	**l**	4359	4016	4561	4395	3116	4065	3420	4207	4341	4125	4037 ± 412
	r	4239	3897	4250	4310	3233	4083	3496	4150	4511	3970	
CA2/3	**l**	2226	2164	2133	2185	1430	1992	1577	2130	2261	2195	

	r	2234	1941	1918	2211	1575	2006	1826	2141	2517	2150	2041 ± 267
DG	l	3669	3184	3363	3608	2534	3256	2791	3163	3561	3598	3266 ± 359
	r	3480	3173	3328	3724	2570	3317	2767	3199	3679	3357	
V1	l	2085	1708	2155	1904	1401	1710	1634	1927	1973	1832	1828 ± 206
	r	1992	1751	2118	1796	1498	1647	1607	1963	1967	1884	

Table 9 Quantitative receptor densities of $mGlu_{2/3}$ [fmol/ mg protein] in brain regions of wild type mice (wt) (l=left and r=right hemisphere). Mean ± standard deviation calculated.

$mGlu_{2/3}$	**Animal**	**11**	**12**	**18**	**22**	**23**	**27**	**28**	**33**	**39**	**Mean ± SD**
	Group	**wt**	**wt**	**wt**	**wt**	**wt**	**wt**	**wt**	**wt**	**wt**	
OB	**l**	3422	3534	3985	3876	3613	3510	4391	3652	4507	3812 ± 387
	r	3352	3399	3822	3744	3660	3633	4414	3607	4491	
M1	**l**	5303	6949	5737	4730	5510	4177	5581	4788	5629	5391 ± 802
	r	5396	7324	5486	4936	5576	4219	5704	4661	5338	
S1	**l**	5424	6582	6420	5414	6311	4390	5614	5161	5388	5631 ± 708
	r	5430	6969	5356	5460	5885	4461	6576	5045	5478	
CPu	**l**	3877	5047	4373	3453	3707	2939	3971	3565	3813	3824 ± 538
	r	3888	4817	4044	3671	3769	2903	3876	3403	3720	
CA1	**l**	1681	2295	2156	2854	2389	1547	3398	3154	1999	2343 ± 598
	r	1760	2037	1993	2612	2699	1486	3382	2722	2011	
CA2/3	**l**	1438	1497	1642	1986	1775	1449	2799	2021	1607	1728 ± 385
	r	1283	1312	1638	1686	1741	1323	2368	1858	1680	

DG	**l**	4098	6138	5253	5855	6269	4326	7438	5359	4114	5365 ± 1076
	r	3824	5787	5128	5687	6148	4415	7395	4937	4401	
V1	**l**	6856	6685	6931	6463	7089	5523	7620	5167	4931	6405 ± 912
	r	6311	7150	6517	6910	6740	5229	8141	5859	5171	
Cb	**l**	1708	1894	1899	2317	1858	1648	2664	1932	2354	2000 ± 311
	r	1761	1855	1862	2043	1826	1657	2621	1837	2257	

Table 10 Quantitative receptor densities of $mGlu_{2/3}$ [fmol/ mg protein] in brain regions of *Crybb2* mutants (l=left and r=right hemisphere). Mean ± standard deviation calculated.

$mGlu_{2/3}$	**Animal**	**1**	**10**	**13**	**29**	**32**	**34**	**36**	**37**	**40**	**41**	**Mean ± SD**
	Group	**Crybb2**	**Crybb2**	**Crybb2**	**Crybb2**	**Crybb2**	**Crybb2**	**Crybb2**	**Crybb2**	**Crybb2**	**Crybb2**	
OB	**l**	2957	3807	3962	3980	4424	3966	4503	4029	4436	3850	3978 ± 447
	r	2889	3868	4217	4040	4675	3749	4219	4109	4210	3666	
M1	**l**	5926	6567	5930	5972	6536	5691	4220	5285	7215	5794	5932 ± 802
	r	6259	6463	6329	6462	6351	5453	4199	4886	6933	6164	
S1	**l**	5553	6671	6218	5787	6830	6096	4810	5019	7468	5844	5901 ± 729
	r	5657	6318	6418	6275	6472	5406	4812	4714	5569	6084	
CPu	**l**	4371	4281	4343	4460	4741	3933	3400	3566	5415	4021	4185 ± 549
	r	4439	4323	4423	4427	4318	3925	3135	3291	4859	4031	
CA1	**l**	2457	2879	2609	2409	3540	2707	2244	2363	3911	2327	2737 ± 519
	r	2584	2840	2518	2422	3597	2556	2294	2501	3688	2283	
CA2/3	**l**	1897	2047	2089	1875	2678	1810	1813	1708	2698	2036	

Raw data

	r	1809	1795	2065	2002	2933	1805	1952	1730	2487	2133	2068 ± 353
DG	l	5706	6046	5706	5338	5918	5905	5528	4580	6165	5003	5530 ± 533
	r	5496	6363	5635	4875	5998	5862	5549	4423	5660	4855	
V1	l	7271	6815	6740	6608	6649	6943	6435	5154	7794	5278	6599 ± 867
	r	6858	7369	7095	5497	8090	6256	6574	5539	7682	5339	
Cb	l	1869	1826	2125	2205	2637	1691	1865	1570	2502	1949	2009 ± 337
	r	1641	2005	2007	1980	2702	1664	1931	1608	2442	1951	

Table 11 Quantitative receptor densities of $GABA_A$ [fmol/ mg protein] in brain regions of wild type mice (wt) (l=left and r=right hemisphere). Mean ± standard deviation calculated.

$GABA_A$	Animal	11	12	18	22	23	27	28	33	39	Mean ± SD
	Group	wt	wt	wt	wt	wt	wt	wt	wt	wt	
OB	l	2308	4122	3020	2785	2291	2629	2851	3994	2987	3052 ± 620
	r	2268	4142	2680	2735	2330	2567	2779	3831	3084	
M1	l	1684	2888	2169	1697	1814	2233	2219	2342	1941	2232 ± 406
	r	1693	2747	2451	1533	1816	2353	2814	2596	2090	
S1	l	1854	3350	2556	2688	2722	2673	2723	3304	2468	2826 ± 344
	r	2167	3146	2621	2271	2481	2994	2710	3362	3146	
CPu	l	615	1212	898	946	778	910	1165	1119	923	984 ± 154
	r	637	926	828	912	768	951	1253	1187	973	
CA1	l		2241	2255	1945	2976	2282	1832	2641	2315	2256 ± 349

Raw data

	r		2056	2156	1890	2637	2591	1686	2518	2256	
CA2/3	l		906	936	906	1052	889	847	1170	831	962 ± 162
	r		1314	898	890	880	951	801	996	956	
DG	l		1947	2167	1864	2402	2038	1491	2471	2238	1999 ± 307
	r		1721	2017	1868	2104	2159	1458	2277	2083	
V1	l	1711	3315	3092	2337	2658	3368	2909	3166	3692	3040 ± 412
	r	2105	2815	3249	2360	2894	3331	2647	3706	3108	
Cb	l	3836	5941	4971	5431	3686	4413	3438	5090	5389	4861 ± 831
	r	2948	6126	4588	5530	4243	4643	3520	5492	5274	

Table 12 Quantitative receptor densities of $GABA_A$ [fmol/ mg protein] in brain regions of *Crybb2* mutants (l=left and r=right hemisphere). Mean ± standard deviation calculated.

$GABA_A$	**Animal**	**1**	**10**	**13**	**29**	**32**	**34**	**36**	**37**	**40**	**41**	**Mean ± SD**
	Group	**Crybb2**	**Crybb2**	**Crybb2**	**Crybb2**	**Crybb2**	**Crybb2**	**Crybb2**	**Crybb2**	**Crybb2**	**Crybb2**	
OB	l	2221	1936	2426	2304	2419	2117	2679	2590	3095	2845	4861 ± 831
	r	2006	1971	2270	2173	2364	2129	2498	2681	3244	3212	
M1	l	1678	1553	2396	1686	2405	1584	2038	1867	2892	2348	2040 ± 472
	r	1793	1581	2417	1696	2413	1401	1731	1835	3076	2409	
S1	l	1746	1904	2875	2263	2342	2304	2639	2471	3337	2689	2369 ± 458
	r	2381	1812	2611	2140	2336	2213	2426	2175	3260	1454	
CPu	l	613	513	1149	715	1036	562	852	882	1238	996	836 ± 232

	r	720	516	1026	698	1039	510	765	812	1198	870	
CA1	l	1731	1197	2050	1801	1646	1965	1763	1936	2431	2128	1832 ± 330
	r	1670	1233	1812	1720	1604	1997	1731	2004	2490	1961	
CA2/3	l	963	432	970	765	662	873	813	1276	1036	1028	848 ± 223
	r	761	446	1304	787	639	865	812	914	924	843	
DG	l	1581	1086	1970	1609	1655	2036	1902	2052	2207	2003	1806 ± 357
	r	1579	1135	2059	1566	1576	2153	1790	2145	2436	1775	
V1	l	1946	3497	2634	2697	2070	2500	2560	2509	3918	2685	2839 ± 619
	r	2434	4167	2848	2748	1863	3264	3175	2578	3720	2911	
Cb	l	5070	4166	6099	4885	3481	5367	5335	4165	4676	3727	4715 ± 752
	r	4815	4133	5906	5428	3759	5537	5106	4278	4762	3892	

Table 13 Quantitative receptor densities of BZ binding sites [fmol/ mg protein] in brain regions of wild type mice (wt) (l=left and r=right hemisphere). Mean ± standard deviation calculated.

BZ	**Animal**	**11**	**12**	**18**	**22**	**23**	**27**	**28**	**33**	**39**	**Mean ± SD**
	Group	**wt**	**wt**	**wt**	**wt**	**wt**	**wt**	**wt**	**wt**	**wt**	
OB	l	7207	8072	6541	6227	5527	6060	6689	7408	5792	6590 ± 733
	r	6759	7909	6468	6156	5845	6122	6699	7253	5893	
M1	l	5142		4423	5435	4614	4494	5179	5266	4017	4843 ± 509
	r	5041		4515	5649	4827	4502	5363	5107	3910	
S1	l	5874	6591	5186	6008	5115	5186	5145	5686	4390	5446 ± 591
	r	5608	6583	5184	5855	5032	5121	4900	5749	4815	

Raw data

CPu	**l**	1432		1249	1691	1416	1265	1302	1556	892	1331 ± 224
	r	1387		1180	1655	1422	1256	1260	1437	895	
CA1	**l**	6859	7233	5368	7042	5885	6045	5340	6191	4997	6082 ± 888
	r	6676	7808	4944	7118	5919	6199	5082	5901	4865	
CA2/3	**l**	4152	5174	3533	3930	3721	3695	3357	4044	3004	3786 ± 594
	r	4039	4842	3204	4308	3606	3892	2999	3542	3108	
DG	**l**	5937	7104	4711	5950	4757	4613	4334	5174	4207	5170 ± 997
	r	5998	7168	4528	6304	4610	4708	3911	4926	4126	
V1	**l**	5259	5402	5028	5812	6237	5780	6705	6137	4122	5636 ± 667
	r	5546	5744	5524	5797	5918	6129	6372	5707	4236	
Cb	**l**	2378	2130	2304	2388	2436	2157	2222	2671	1959	2306 ± 190
	r	2433	2162	2373	2462	2493	2151	2175	2557	2053	

Table 14 Quantitative receptor densities of BZ binding sites [fmol/ mg protein] in brain regions of *Crybb2* mutants (l=left and r=right hemisphere). Mean ± standard deviation calculated.

BZ	**Animal**	**1**	**10**	**13**	**29**	**32**	**34**	**36**	**37**	**40**	**41**	**Mean ± SD**
	Group	**Crybb2**	**Crybb2**	**Crybb2**	**Crybb2**	**Crybb2**	**Crybb2**	**Crybb2**	**Crybb2**	**Crybb2**	**Crybb2**	
OB	**l**	7437	6741	6684	8272	8445	6271	6159	5944	5067	6685	6660 ± 973
	r	7273	6556	6412	7851	7905	6150	6019	5756	4864	6712	
M1	**l**	5117	4917	5072	6655	6487	5499	4490	5213	2981	5693	5218 ± 967
	r	5380	4858	5072	6828	5848	5479	4768	5131	3123	5755	
S1	**l**	6393	5213	5884	6375	6554	5692	5181	5356	3518	6042	

Raw data

	r	5886	5369	5418	6704	6036	5862	5009	5434	3529	5870	5566 ± 843
CPu	l	1736	1400	1688	2085	2073	1598	1482	1549	902	1822	1607 ± 334
	r	1616	1299	1572	2225	1858	1655	1403	1482	954	1737	
CA1	l	6736	5081	6018	5288	6664	6062	5060	6953	4702	6450	5833 ± 799
	r	6621	5141	5924	5716	6458	6020	4843	6716	4155	6062	
CA2/3	l	4412	3045	3898	3467	4638	3810	3588	4410	2910	4384	3831 ± 649
	r	5156	3315	3764	3718	4425	3843	3251	3922	2472	4196	
DG	l	6708	4968	5850	5079	5862	5493	4849	6147	3901	5991	5444 ± 828
	r	6916	5049	5788	5057	5791	5156	4776	6045	3593	5862	
V1	l	6227	5745	4959	6351	5981	6128	5728	6279	3576	5470	5677 ± 815
	r	6169	5387	5101	6388	6280	6243	5766	6684	3919	5162	
Cb	l	2244	1855	2231	2396	2680	2384	2184	2535	1428	2092	2192 ± 350
	r	2102	2132	2062	2293	2714	2368	2243	2591	1432	1881	

Table 15 Quantitative receptor densities of $GABA_B$ [fmol/ mg protein] in brain regions of wild type mice (wt) (l=left and r=right hemisphere). Mean ± standard deviation calculated.

$GABA_B$	**Animal**	**11**	**12**	**18**	**22**	**23**	**27**	**28**	**33**	**39**	**Mean ± SD**
	Group	**wt**	**wt**	**wt**	**wt**	**wt**	**wt**	**wt**	**wt**	**wt**	
OB	l	806	633	592	805	610	571	469	732	491	629 ± 107
	r	708	661	561	772	605	606	459	683	558	
M1	l	1491	1393	1379	1471	1535	1407	1122	1917	1244	1462 ± 219
	r	1505	1426	1258	1479	1517	1478	1212	2019	1466	

Raw data

S1	**l**	1439	1215	1236	1436	1345	1202	1090	1657	1175	1308 ± 184
	r	1313	1311	1221	1505	1211	1217	1050	1735	1183	
CPu	**l**	953	715	718	922	821	654	677	922	636	778 ± 119
	r	899	819	675	882	821	678	637	935	648	
CA1	**l**	1418	1269	1123	976	1028	1054	868	1455	1127	1171 ± 179
	r	1339	1253	1088	1270	1178	1045	942	1490	1154	
CA2/3	**l**	1681	1411	1416	1774	1492	1434	1177	1792	1406	1502 ± 200
	r	1682	1472	1311	1703	1569	1364	1117	1765	1476	
DG	**l**	1665	1546	1280	1745	1414	1281	1129	1745	1436	1470 ± 205
	r	1591	1533	1249	1690	1469	1286	1189	1777	1424	
V1	**l**	1573	1511	1553	1746	1426	1482	1396	1904	1322	1524 ± 179
	r	1544	1376	1469	1714	1445	1324	1258	1839	1558	
Cb	**l**	1527	1598	1362	1843	1268	1435	1413	1735	1445	1518 ± 164
	r	1473	1484	1580	1823	1358	1472	1374	1700	1439	

Table 16 Quantitative receptor densities of $GABA_B$ [fmol/ mg protein] in brain regions of *Crybb2* mutants (l=left and r=right hemisphere). Mean ± standard deviation calculated.

$GABA_B$	**Animal**	**1**	**10**	**13**	**29**	**32**	**34**	**36**	**37**	**40**	**41**	**Mean ± SD**
	Group	**Crybb2**	**Crybb2**	**Crybb2**	**Crybb2**	**Crybb2**	**Crybb2**	**Crybb2**	**Crybb2**	**Crybb2**	**Crybb2**	
OB	**l**	731	803	554	749	484	771	512	621	771	565	660 ± 120
	r	759	783	574	738	478	810	536	609	797	562	

Raw data

M1	**l**	1608	951	1459	1418	1628	1766	1343	1429	1988	1835	1550 ± 272
	r	1587	1121	1442	1385	1402	1832	1479	1470	2007	1845	
S1	**l**	1462	1185	1302	1281	1304	1594	1137	1278	1669	1476	1368 ± 170
	r	1404	1174	1279	1329	1286	1570	1153	1283	1706	1481	
CPu	**l**	896	644	797	813	728	891	685	752	983	860	804 ± 104
	r	873	697	752	766	678	990	712	744	945	872	
CA1	**l**	1409	1298	977	1231	1086	1382	1066	1226	1536	1320	1264 ± 160
	r	1416	1208	1322	1133	1151	1412	1020	1243	1537	1301	
CA2/3	**l**	1680	1606	1646	1534	1489	1782	1354	1570	2144	1701	1633 ± 197
	r	1733	1487	1649	1539	1524	1810	1263	1624	1964	1568	
DG	**l**	1685	1569	1605	1519	1452	1761	1302	1538	1876	1617	1583 ± 172
	r	1680	1437	1601	1396	1500	1777	1250	1519	1895	1682	
V1	**l**	1785	1492	1400	1949	1761	1971	1555	1691	1954	1854	1741 ± 172
	r	1756	1633	1569	1902	1728	1951	1519	1672	1778	1902	
Cb	**l**	1111	1437	1300	1594	1503	1729	1512	1458	1449	1470	1465 ± 157
	r	1456	1478	1166	1698	1444	1713	1479	1428	1522	1349	

Table 17 Quantitative receptor densities of $D_{2/3}$ [fmol/ mg protein] in striatum of wild type mice (wt) (l=left and r=right hemisphere). Mean ± standard deviation calculated.

$D_{2/3}$	**Animal**	**11**	**12**	**18**	**22**	**23**	**27**	**28**	**33**	**39**	**Mean ± SD**
	Group	**wt**	**wt**	**wt**	**wt**	**wt**	**wt**	**wt**	**wt**	**wt**	

Raw data

CPu	**l**	3129	3442	2677	2688	3076	3058	3366	3838	2899	3095 ± 340
	r	3229	3275	2689	2636	2881	3043	3148	3680	2965	

Table 18 Quantitative receptor densities of $D_{2/3}$ [fmol/ mg protein] in striatum of *Crybb2* mutants (l=left and r=right hemisphere). Mean ± standard deviation calculated.

$D_{2/3}$	**Animal**	**1**	**10**	**13**	**29**	**32**	**34**	**36**	**37**	**40**	**41**	**Mean ± SD**
	Group	**Crybb2**	**Crybb2**	**Crybb2**	**Crybb2**	**Crybb2**	**Crybb2**	**Crybb2**	**Crybb2**	**Crybb2**	**Crybb2**	
CPu	**l**	3368	3057	3153	2832	3830	2913	3307	3445	4431	3940	3414 ± 509
	r	3505	3119	3070	2780	3911	2680	3311	3313	4395	3920	